


## REVIEW OPEN ACCESS

# High Temperature Shock (HTS) Synthesis of Carbon-Based Nanomaterials for Electrochemical Applications

Wen Huang<sup>1</sup> | Xindong Zhu<sup>1</sup> | He Zhu<sup>1</sup> | Zhihua Wang<sup>1</sup> | Haoran Yu<sup>1</sup> | Yu Shao<sup>1</sup> | Qi Liu<sup>2</sup>  | Si Lan<sup>1</sup>

<sup>1</sup>Herbert Gleiter Institute of Nanoscience, School of Materials Science and Engineering, Nanjing University of Science and Technology, Nanjing, China | <sup>2</sup>Department of Physics, City University of Hong Kong, Kowloon, China

**Correspondence:** He Zhu ([hezhu@njust.edu.cn](mailto:hezhu@njust.edu.cn)) | Yu Shao ([yushao2024@126.com](mailto:yushao2024@126.com)) | Si Lan ([lansi@njust.edu.cn](mailto:lansi@njust.edu.cn))

**Received:** 16 October 2024 | **Revised:** 18 November 2024 | **Accepted:** 15 December 2024

**Funding:** This study was financially supported by the National Key R&D Program of China (No. 2021YFB3802800), the National Natural Science Foundation of China (Nos. 22275089, 52222104, 12261160364), the Fundamental Research Funds for the Central Universities (No. 30922010307).

**Keywords:** batteries | carbon-based nanomaterials | electrocatalysts | high temperature shock | ultrafast synthesis

## ABSTRACT

Carbon-based nanomaterials play a significant role in the field of electrochemistry because of their outstanding electrical conductivity, chemical and thermal resistance, structural flexibility, and so on. In recent years, we have observed a rapid rise of research interest in the high-temperature shock (HTS) method, which is fast, stable, environmentally friendly, and versatile. The HTS method offers excellent controllability and repeatability while tackling challenges and limitations of traditional preparation methods, providing a new way to prepare and optimize carbon-based nanomaterials for electrochemical applications. During the HTS synthesis, the reaction is driven by the high temperature while further growth of obtained nanoparticles is inhibited by the rapid heating and cooling rates. The preparation of carbon-based nanomaterials by HTS has many advantages, including controlled carbon vacancy that may drive phase transformation, precise engineering of carbon, and other defects that may function as active centers, formation and preservation of metastable phase owing to the high energy and rapid cooling, fine-tuning of the interaction between loaded species and carbon support for optimized performance, and facile doping and compounding to induce synergy between different constituents. This article provides a comprehensive review of various carbon-based nanomaterials prepared by the HTS method and their applications in the field of electrochemistry during the past decade, emphasizing their synthesis and principles to optimize their performance. Studies showcasing the merits of HTS-derived carbon-based nanomaterials in advancing Lithium-ion batteries, Lithium-sulfur batteries, Lithium-air batteries, water-splitting reaction, oxygen reduction reaction, CO<sub>2</sub> reduction reaction, nitrate reduction reaction, other electrocatalytic reactions, and fuel cells are highlighted. Finally, the prospects of carbon-based nanomaterials prepared by HTS method for electrochemical applications are recommended.

## 1 | Introduction

Access to sustainable, affordable, and reliable energy has become paramount in the 21st century [1]. Electrochemistry

offers numerous opportunities in the pursuit of sustainable energy, including its conversion, storage, and utilization [2]. Meanwhile, challenges are encountered particularly due to the lack of appropriate materials in various electrochemical

Wen Huang and Xindong Zhu contributed equally to this study.

This is an open access article under the terms of the [Creative Commons Attribution](https://creativecommons.org/licenses/by/4.0/) License, which permits use, distribution and reproduction in any medium, provided the original work is properly cited.

© 2025 The Author(s). *Carbon Neutralization* published by Wenzhou University and John Wiley & Sons Australia, Ltd.

applications such as hydrogen production via water electrolysis, fuel cells, and batteries. Carbon-based nanomaterials are deemed prospective in resolving these challenges and limitations [3, 4]. Carbon-based nanomaterials significantly contribute to advancements in the energy sector [5], and they have been extensively studied in the last decade. Owing to their outstanding electrical conductivity, affordability, heat, chemical, and radiation resistance, and tunable surface and interfacial properties, carbon-based nanomaterials hold significant promise for various applications [6]. The unique properties of carbon-based nanomaterials impart the following advantages in electrochemical applications [7, 8]: their high electrical conductivity promotes the rapid electron migration and improves the reaction rate at the electrodes; their large specific surface area increases the contact area between the electrodes and the electrolyte, thus improving the charge storage capacity; their stability in various electrochemical environments prolong the service life of the electrodes; their excellent mechanical properties allow them to withstand the mechanical stresses during electrode preparation and usage; lastly, the optimization of their electrochemical properties can be achieved by altering their structures [9–15].

Carbon-based nanomaterials have been prepared by many traditional methods, such as chemical vapor deposition (CVD) [16], spray drying [17], hydro and solvothermal methods [18], and electrodeposition [19]. Conventional methods for synthesizing carbon-based nanomaterials typically require extended thermal treatments with low heating rates to achieve fine crystal structures. However, these approaches often encounter several challenges, including complex reaction processes, slow kinetic rates, intricate operating conditions, time-consuming protocols, limited control over crystal structures, high cost, and constraints related to substrates and coatings [20, 21] (Table 1). For example, while CVD is widely used for crystal growth at high temperatures, it relies on precisely controlled reaction conditions including gas composition and reaction duration. In addition, CVD usually requires the use of expensive precursors, such as metal-organic compounds in metal-organic vapor deposition (MOCVD), elevating cost and operational complexity [22, 23]. Spray drying, another common preparation method known for its excellent performance in preparing large-area homogeneous films, may result in poor crystal quality and poor nanostructural uniformity of the product when it is performed under unconventional reaction conditions [24–26]. Similarly, while hydrothermal and solvothermal methods are capable of

producing nanoparticles at lower temperatures, there is a subtle balance between the modulation of reaction conditions and the obtained product structure, limiting their large-scale application [27, 28]. Lastly, although conventional electrodeposition methods excel in obtaining electrodes with complex, desired shapes, their application is limited by drawbacks including the incapability to obtain desired nonuniformity, the narrow range of electrode surfaces or coating substrates selections, difficult optimization of material properties, and poor long-term stability of the obtained electrodes. Therefore, current research continues to explore new processing techniques to overcome these limitations and to further enhance the performance of carbon-based nanomaterials in electrochemical applications.

In recent years, a new method for ultrafast nanomaterial synthesis, high temperature shock (HTS), has emerged, which mainly includes Joule heating, microwave heating, and laser irradiation. HTS presents several significant advantages over conventional methods: (1) HTS is highly user-friendly and supports rapid synthesis. The material can quickly reach elevated temperatures, which accelerates chemical reactions, significantly reduces synthesis time, and enhances productivity. (2) HTS has fewer stringent requirements for substrates and precursors. It can be synthesized using a wide range of readily available materials, which not only lowers production costs but also increases the adaptability of the technique. (3) HTS provides exceptional control over structural properties. By finely tuning the synthesis parameters and reaction conditions, the structures of nanomaterials can be customized to achieve specific desired characteristics. (4) Nanomaterials synthesized via the HTS method typically exhibit enhanced stability. The rapid heating and cooling associated with HTS minimizes structural defects and phase transitions during the synthesis process. This contributes to the improved stability and reliability of the resulting nanomaterials. Overall, various nanomaterials have been prepared using HTS and are widely applied in various fields [29]. In particular, for the preparation of carbon-based nanomaterials, HTS technology gives full play to the advantages of carbon-based nanomaterials. Carbon-based nanomaterials with specific morphology and structure can be synthesized by appropriate adjustments of the synthesis conditions [30]. Therefore, compared to traditional methods, HTS not only has fast reaction time, simple operation, cost savings, and fewer limitations on substrates and coatings, but more importantly, it is more conducive to structural control. Of course, HTS also has some shortcomings, such as synthesis being too fast to study the reaction process, difficulty in large-scale production, and so on.

**TABLE 1** | Comparison of HTS technology and other methods for synthesizing carbon-based nanomaterials.

	CVD	SD	HSTM	ED	HTS
Time level	Hours	Minutes	Hours	Hours	Milliseconds
Heating rate ( $\text{k s}^{-1}$ )	< 10	< 10	< 10	< 10	> $10^5$
Cost	High	Middle	Middle	Middle	Low
Environment-friendliness	Low	Middle	Middle	Middle	High
Energy consumption	High	Middle	Middle	Middle	Low
Particle dispersity	Middle	Low	Middle	Low	High
Particle miscibility	Low	Low	Middle	Low	High

Carbon-based materials effectively disperse deposited species and are favorable for the generation of ultra-small nanoparticles during the HTS synthesis. These obtained ultra-small nanoparticles usually possess higher surface energy, more active sites, improved electron transport efficiency, and higher ion diffusion rate, thus further improving the charge storage and transport properties of nanomaterials [31]. HTS method's capability of fine-tuning the obtained nanoparticle structure, such as synthesizing rare substable phases, as well as its enhancement of those inherent advantages of the carbon materials, including high specific surface area, superb electrical conductivity, and so on, altogether make carbon-based nanomaterials prepared by HTS method promising candidates for electrochemical applications toward a sustainable energy future [32].

Accordingly, the synthesis of carbon-based nanomaterials using HTS has become a hot topic in recent years and has led to outstanding achievements in the field of electrochemistry. In this report, the history of the HTS method development, the necessary instrument, the synthesis process, the heating principle, the

temperature measurement principle, and the synthesis mechanism of carbon-based nanomaterials by HTS are described. The HTS-synthesized carbon-based nanomaterials, as well as their application and optimization in the field of energy-related electrochemistry are comprehensively discussed (Figure 1).

## 2 | Principles and Methods of HTS Technology

### 2.1 | Heating Principle of HTS

HTS technique utilizes heat generated when an electric current passes through a conductor. In a typical synthesis, the reaction zone temperature can be raised instantaneously ( $10^5 \text{ K s}^{-1}$ ) to thousands of Kelvin and get cooled down in milliseconds (Figure 2a). At present, HTS syntheses are mainly performed with Joule ultra-fast heating equipment (Figure 2b) and Joule flash heating equipment (Figure 2c). A common setup mainly consists of four parts: a heating reaction chamber, a spectrometer, a DC power supply, and a vacuum pump. The heating process is based on Joule's law. The operator enjoys the freedom to adjust the current, voltage, and the

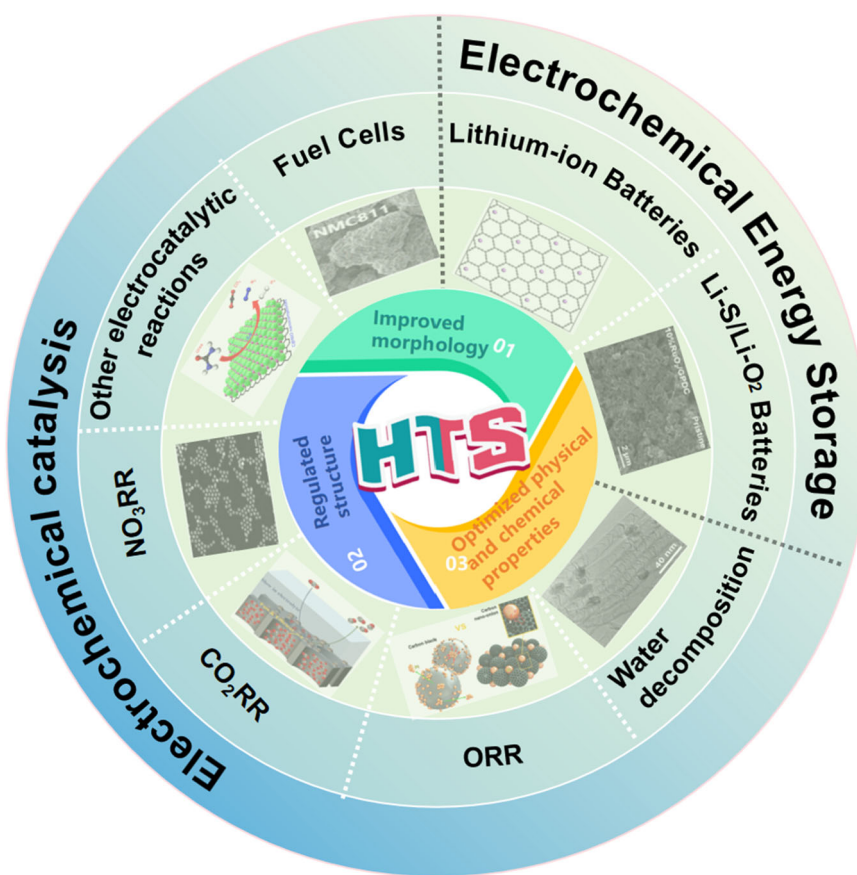


**FIGURE 1** | Overview of HTS synthesis derived carbon-based materials and their applications in various electrochemical processes: lithium-ion battery. (Inset: Atomic structures of a Li atom attached on  $2 \times 2$   $\alpha$ -graphene. Reproduced with permission: Copyright 2013, American Chemical Society [33]. The SEM image of the 10%  $\text{RuO}_2/\text{GPDC}$ . Reproduced with permission: Copyright 2021, American Chemical Society [34]. The TEM image shows N-CNTs with encapsulated Fe nanoparticles. Reproduced with permission: Copyright 2018, American Chemical Society [35]. Schematic diagram of nanoparticles loaded on carbon black. Reproduced with permission: Copyright 2017, American Chemical Society [36]. The proposed mechanistic pathways of  $\text{CO}_2\text{RR}$  over the 20% $\text{Au}/\text{FPC-800}$  electrocatalyst. Reproduced with permission: Copyright 2023, American Chemical Society [37]. Low-magnification HAADF-STEM image of Cu NP TDPA showing the sample monodisperse nature. Reproduced with permission: Copyright 2024, American Chemical Society [38]. Schematic diagram of urea oxidation of carbon-based materials. Reproduced with permission: Copyright 2021, American Chemical Society [39]. The SEM image of the NMC811. Reproduced with permission: Copyright 2019, American Chemical Society [40].

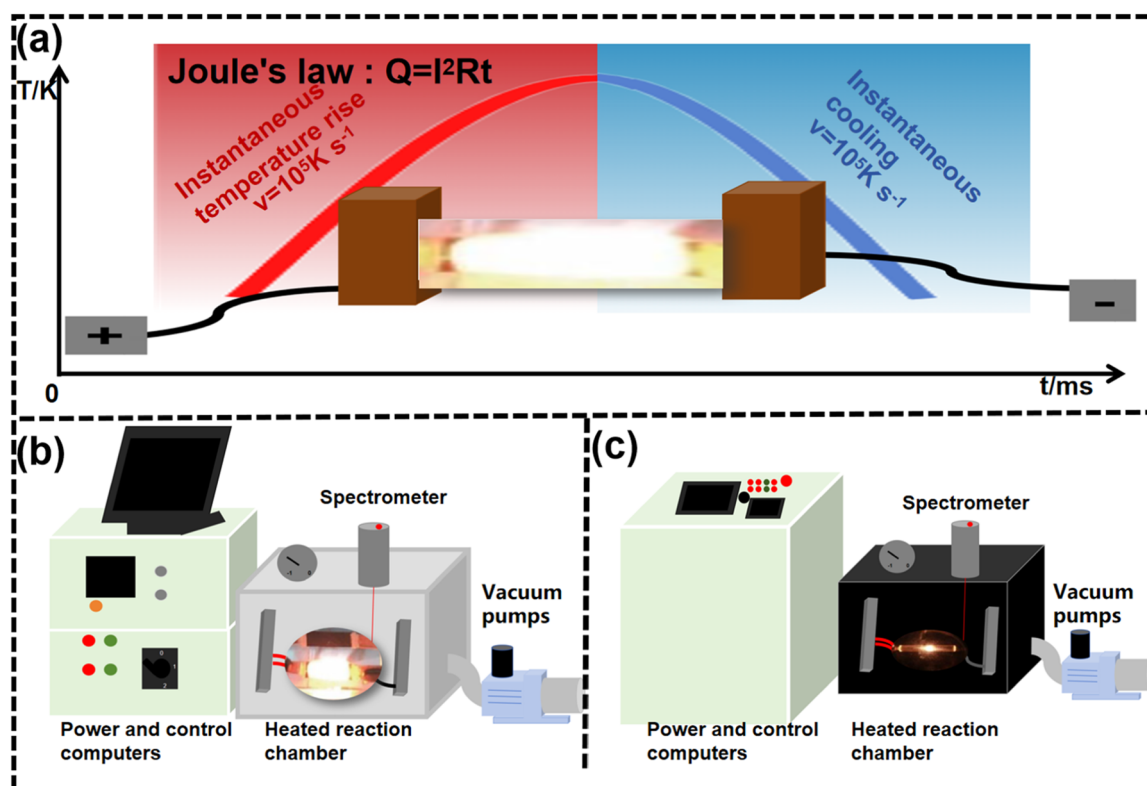


**FIGURE 2** | (a) Principles and processes of HTS. (b) Joule ultra-fast heating equipment. (c) Joule flash heating equipment.

conductor resistance, individually or simultaneously, such that the temperature profile during the synthesis can be well customized. It should be noted that the accuracy of temperature control for Joule heating is related to the following factors: (1) the heat capacity of the conductor: the larger the heat capacity, the slower the temperature change, the lower the control accuracy; (2) the heat loss during synthesis: the more heat loss, the lower the control accuracy [41]; (3) the temperature sensor accuracy: the higher the accuracy of the temperature sensor, the higher the control accuracy.

## 2.2 | Principles and Methods of HTS Synthesis for Optimization of Carbon-Based Nanomaterials

HTS technology can directly prepare high-performance carbon nanomaterials including carbon nanofibers (CNFs), carbon nanotubes (CNTs), reduced graphene oxide (RGO), carbon-based nanomaterials from biomass (carbon-willow branches and lignocellulosic carbon), and 3D-printed carbon-based materials, among others [42]. HTS also enables the facile preparation of carbon-based nanomaterials, by heating precursors and self-supporting matrices combined through facile pre-treatments (Figure 3). The excellent electron transfer ability and corrosion resistance make carbon materials an ideal carrier for metal nanoparticles. Two major categories of metal precursors are generally used: (1) micron-sized solids and (2) metal salt solutions. The carbon materials show good affinity toward anchoring the nanoparticles, thus preventing the aggregation of nanoparticles. The interaction between metal and carbon material substrates can greatly improve the activity and stability of derived catalysts [44].

Lately, researchers have carried out ultrahigh-temperature treatment of carbon-based nanomaterials by HTS technology, aiming at modulating the structure, engineering the morphology, and enhancing the physical and chemical properties of obtained materials. The ultrahigh-temperature treatment of carbon-based nanomaterials using the HTS technique significantly improves their physical and chemical properties. This includes enhanced graphitization, as well as increased thermal and electrical conductivity, alongside improved thermal stability. The improvements arise from the optimization of vacancies, residual oxygen-containing functional groups, carbon defects, and various other defects. The high-temperature conditions during HTS facilitate the migration and rearrangement of carbon atoms, leading to the formation of carbon vacancies [45, 46]. The presence of these vacancies alters the electronic structure of the material, which in turn affects its electrical and thermal conductivity [47]. Besides, the HTS process can also induce and modulate other types of defects, including grain boundaries, stresses, etc. Defects in the material can significantly influence its physical and chemical properties [48, 49]. Therefore, by controlling the synthetic parameters like temperature, duration, and atmosphere during HTS, we can precisely regulate the structure and surface chemistry of obtained materials, giving them desired properties and prospects as functional materials in the fields of material, electrochemistry, and energy.

For instance, RGO can be obtained when graphene oxide (GO), a graphene monolayer with various oxygen-containing functional groups, is reduced thermally, chemically, electrochemically, or photochemically. RGO comprises ordered  $sp^2$  domains interspersed with nanoscale structures within a



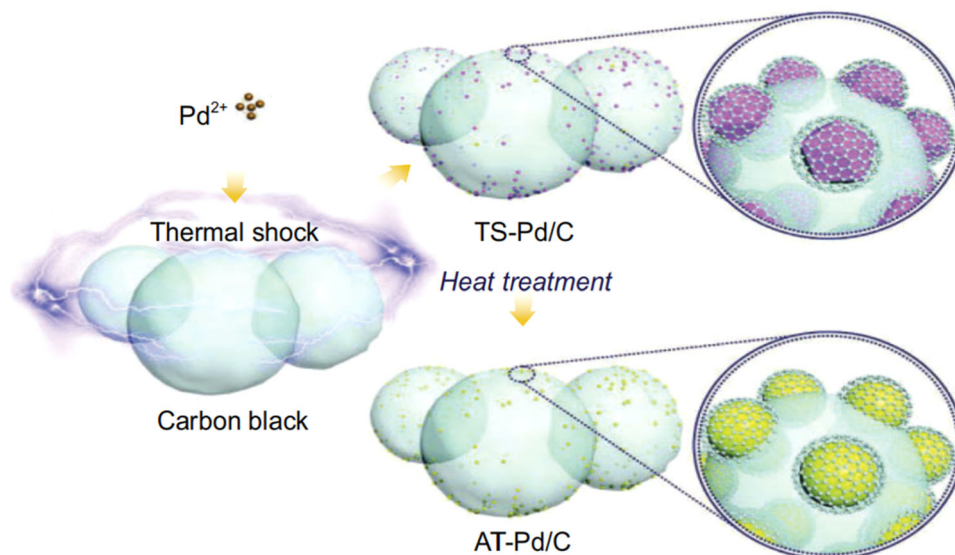


**FIGURE 3** | Fabrication of metastable monometallic nanostructures. Reproduced under terms of the CC-BY license [43]. Copyright 2024, Xiaoya Cui et al., published by Oxford University Press on behalf of China Science Publishing & Media Ltd.

disordered  $sp^3$  matrix, which contains oxygen-functional groups. The presence of vacancies, residual oxygen groups, and various defects in RGO films can effectively scatter or trap charge carriers traversing the  $sp^2$  lattice, consequently limiting the films' charge mobility and electrical conductivity. However, Profs. Yilin Wang, Yanan Chen, and Liangbing Hu used the HTS method to prepare RGO films at 3000 K, achieving record-breaking high conductivity and carrier mobility (Figure 4). A more compact structure reduced the defects and impurities, along with an increased specific surface area, enhances conductivity and charge mobility [50].

Second, HTS technology with its ultra-fast heating/cooling rates also allows for efficient regulation of particle size and dispersion [51]. The rapid reaction speed of HTS limits the growth of the formed nanoparticles, thus containing them at the nanometer scale. On the other hand, the dispersion of nanoparticles formed during HTS is mainly regulated by the "hindered agglomeration method" and the "anchored growth method." The "hindered agglomeration method" relies on an in situ generated solid or gas overlayer on the particle surface to hinder the agglomeration of nanoparticles. At the start, HTS induces highly exothermic chemical reactions by providing the necessary energy externally during the rapid thermal shock. Localized reactions occur within the system to form chemical reaction fronts (combustion waves), which then proceed rapidly, supported by its own exothermic heat, to spread the combustion waves throughout the system. The reaction heat rapidly decomposes the precursor and releases a large amount of gas, which prevents the agglomeration and growth of formed nanoparticles. Volatile impurities are removed by evaporation when the system reaches high temperatures of several thousand degrees in an instant. The elevated temperatures experienced during thermal shock can result in particle coarsening. However, extremely high temperatures may facilitate the "fission" and "fusion" of metal precursors, resulting in a uniform mix of elements. Additionally, rapid cooling rates enable effective control of the thermodynamic mixing state and facilitate

the formation of crystalline solid solution nanoparticles. The particle aggregation and phase separation of nanoparticles during high-temperature operation usually hinder their practical feasibility. Ahn et al. reported an oxide coating on the surface of CNFs formed by a simple sol-gel method, and then nanoparticles were rapidly synthesized by thermal shock (Figure 5a-c). The oxide coating hindered the growth and aggregation of the nanoparticles and caused them to root tightly into the oxide coating, achieving ultra-stable electrocatalytic performance [52]. The "anchored growth method" exploits the fact that defect edge planes are the preferred location for the formation and stabilization of metal nanoparticles. Fabricated carbon defects can provide ideal nucleation sites, and the nanoparticles synthesized with HTS are further rooted on the edge planes by inserting metal atoms between the carbon planes, resulting in a stronger interaction between the nanoparticles and the carbon carrier. The study conducted by Hu Liangbin and colleagues investigates the methods for forming and stabilizing metal nanoparticles on carbon-based carriers [57]. CNF immersed in the metal precursor solution produced T-shaped graphite structures with highly defective edge planes due to the high temperature and rapid gas precipitation during Joule heating, producing fine and uniformly distributed nanoparticles.

Due to its fast, convenient, and high-temperature nature, HTS has been applied more frequently to modulate the structure of carbon-based nanomaterials to construct substable materials that are difficult to achieve by conventional methods. Such phase transition may be driven by appropriate thermal shock conditions. Normally, energy input above the stabilization threshold of the original phase results in a phase transition and the formation of a new stable structure. Meanwhile, the presence of carbon vacancies brought about by thermal shock creates a localized energy gradient, lowering the energy barrier for the phase transition and making it more likely to occur. Thereafter, rapid cooling "freezes" the positions of atoms at high temperatures and prevents them from migrating to re-establish the original phase during the rapid cooling, thus

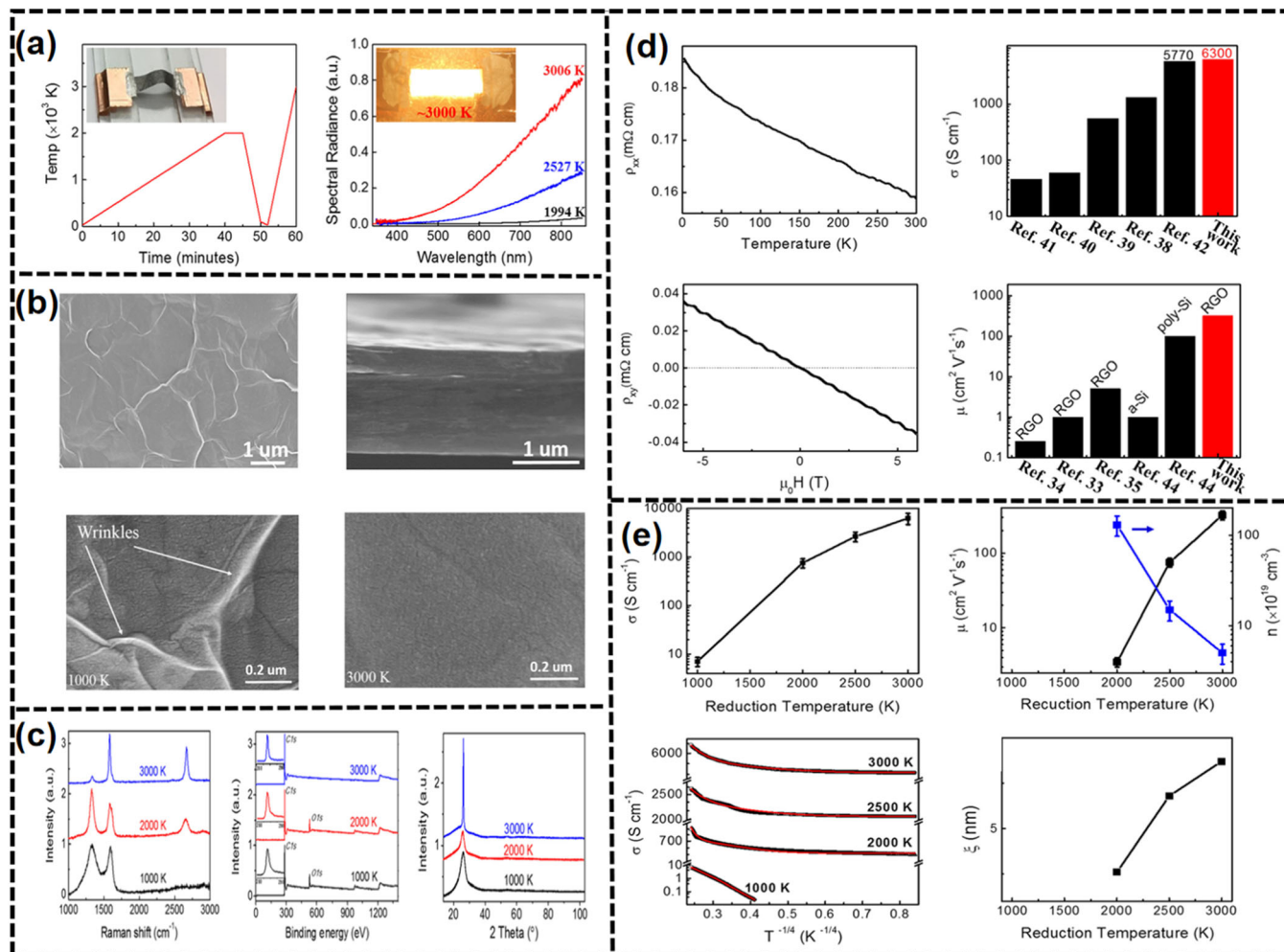


**FIGURE 4** | Ultrahigh-temperature HTS to prepare RGO films with high conductivity and carrier mobility. (a) Generate RGO thin film through Joule heating. (b) SEM images of RGO thin films prepared using different methods and angles. (c) Raman, XPS, and XRD of RGO thin films. (d) Transport properties of the 3000-K-reduced RGO film. (e) The influence of temperature on RGO. Reproduced with permission: Copyright 2018, Elsevier [50].

contributing to the stabilization of substable phases. Higher temperatures provide enough energy to overcome the bonding energy between atoms and cause them to migrate, while longer heating times will cause more atoms to migrate. The unique electronic structure of metastable materials may form channels that are more conducive to rapid electron conduction, and high surface energy creates abundant active sites. And, the flexible structure can better adapt to reaction requirements such as adsorption and desorption. Therefore, it has better electrochemical activity. Deng et al. selectively synthesized phase-pure molybdenum carbides by controlling the pulse voltage of the FJH (Figure 5d) [53]. The diverse energy inputs of FJH facilitate the formation of higher energy fugitive phases that are not thermodynamically stable. Furthermore, the rapid cooling characteristic of the FJH process promotes the kinetic stabilization of these fugitive phases. Simultaneous adjustment of thermal shock temperature and duration makes it convenient for the phase-selective and composition-selective synthesis using the HTS process. Chen et al. synthesized three different fluorinated carbon isomers by FJH (Figure 5e) [54]. Overall, fluorinated amorphous carbon, fluorinated nanodiamond (sp<sup>3</sup>-carbon), fluorinated turbo graphene (sp<sup>2</sup>-carbon), and fluorinated FCC carbon with high crystallinity and polyhedral shapes can be prepared by tailoring the flash conditions. HTS-derived carbon-based

nanomaterials can also be revamped by customizing the composition of loaded species (e.g., metal nanoparticles). Alloy nanoparticles with various compositions exhibit distinct dimensions and kinetic dislocation characteristics during the ultrafast quenching; a certain degree of structural adjustment is sufficient to optimize carbon-based nanomaterials prepared by HTS. For example, the melting point, surface tension, and growth rate of deposited nanoparticles are strongly correlated with the composition of alloying elements, which in turn affect their final shape, dimension, morphology, and so on. Higher proportions of high melting point elements usually result in larger nanoparticles. In addition, different proportions of alloying elements affect the rate of atomic migration, which in turn affects the formation and evolution of kinetic dislocations. A higher proportion of elements with high diffusion coefficients generally results in the formation of more kinetic dislocations. Li et al. synthesized Pt-Ni alloy nanoparticles with different Pt-Ni ratios on carbon carriers using the HTS method, from which the catalyst with optimal performance was obtained (Figure 5f) [55]. The performance of this catalyst is about six times that of commercial Pt/C catalysts.

The high temperatures and rapid heating in the HTS method can improve the microstructure of carbon nanomaterials. For



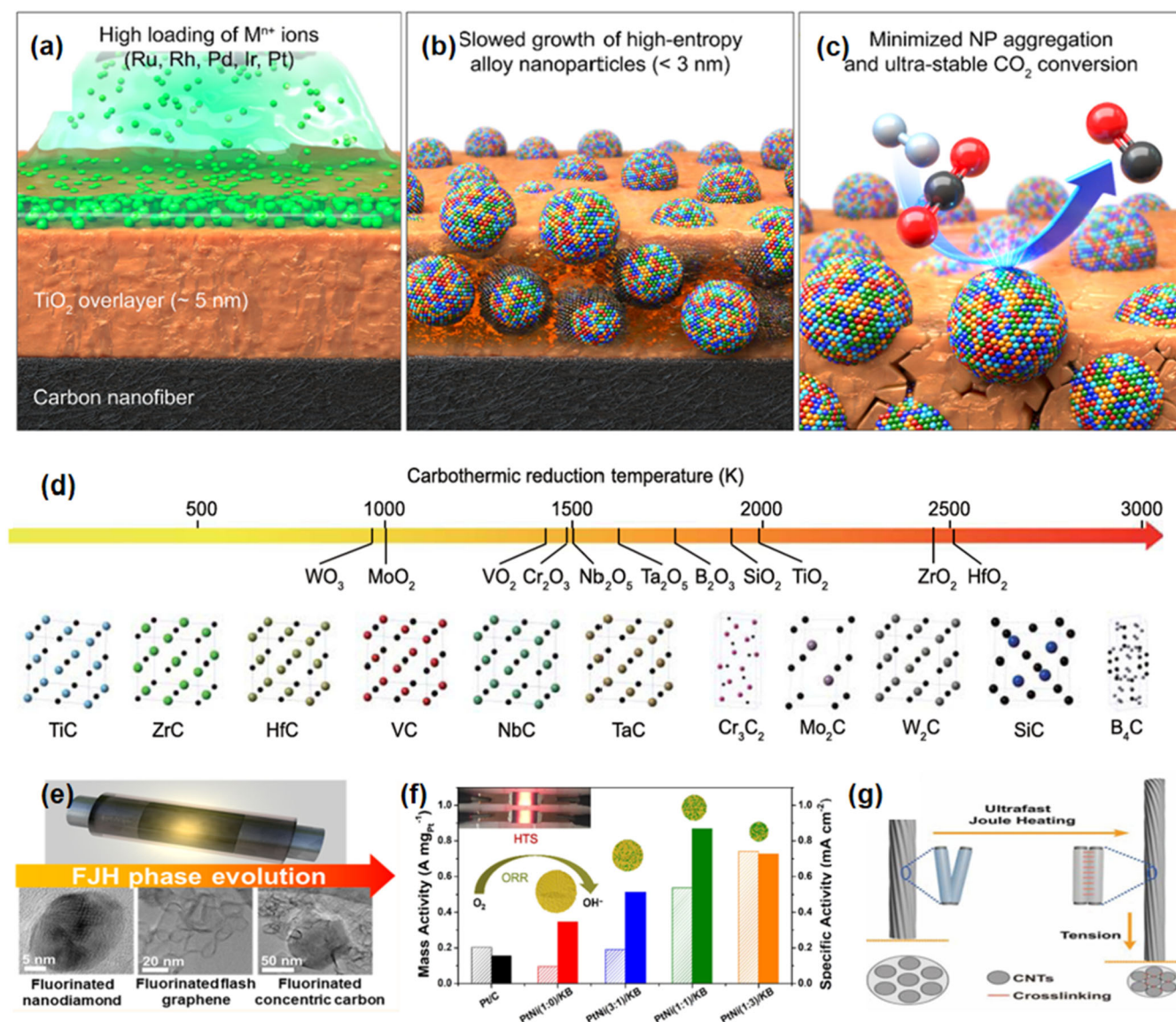


**FIGURE 5** | (a–c) Schematic diagram of using HTS to synthesize HEA, inhibit growth, and apply catalysis. Reproduced with permission: Copyright 2023, American Chemical Society [52]. (d) Carbothermic reduction temperature of oxides derived from the Ellingham diagram, and the crystal structures of 11 carbides. Reproduced under terms of the CC-BY license [53]. Copyright 2022, Bing Deng et al., published by Springer Nature. (e) Phase evolution of carbon materials during FJH. Reproduced with permission: Copyright 2021, American Chemical Society [54]. (f) ORR activities of PtNi nanoparticles. Reproduced with permission: Copyright 2022, American Chemical Society [55]. (g) Schematic illustrations of the welding process of CNT fibers induced by HTS. Reproduced with permission: Copyright 2019, Royal Society of Chemistry [56].

example, lignin-like biomass is converted to highly crystalline graphitic carbon by atomic rearrangement through the Joule heating process. In addition, HTS technique can be employed to induce strong cross-linking and increase the density of CNT fiber that originally has weak or even lack connections between adjacent CNTs, benefited from the tension applied at high temperatures [58]. Song et al. used Joule heating to treat CNT fibers to high temperatures (~2723.15 K) under applied tension (Figure 5g), and rapid stretching and densification of CNT fibers under tension can be achieved in a few milliseconds by applying a high pulse voltage. This is beneficial for improving its conductivity and stability. The rapid synthesis and low cost of the Joule heating method offer great potential for large-scale application of CNT fibers [56].

### 3 | Carbon-Based Nanomaterials Prepared by HTS in Electrochemical Applications

#### 3.1 | Electrochemical Energy Storage (EES)

Availability is the major factor limiting our transition to clean energy. Its effective utilization presupposes energy harvest, storage, and redistribution in the form of electrical energy [59]. With the merit of cost efficiency, environmental friendliness, and high reliability, EES devices have received extensive attention [60]. Hereby, EES devices represented by secondary cells have developed rapidly in recent years [61]. In this section, we introduced the application of HTS in EES.

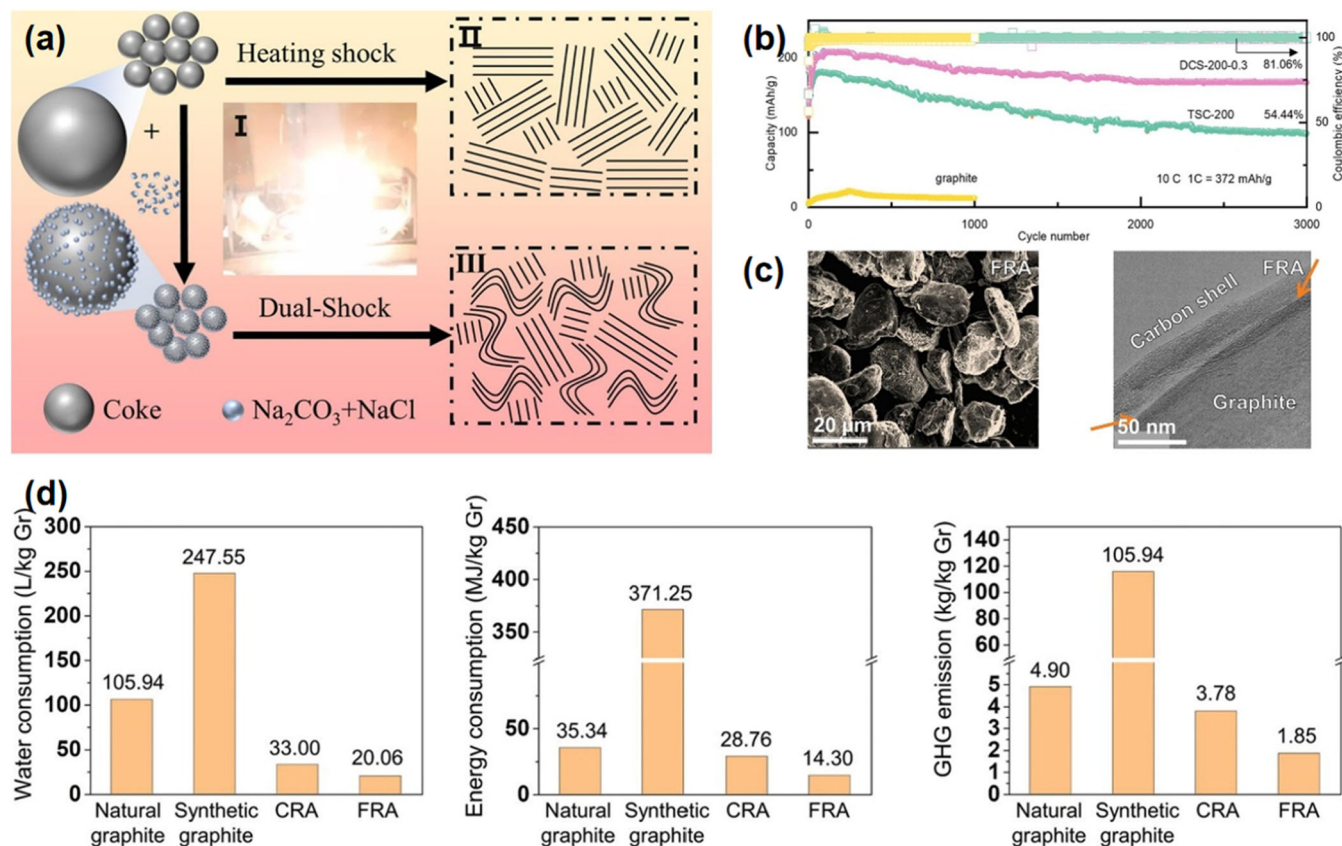


**FIGURE 6** | (a) Schematic comparison of the heating shock and the dual shock. (b) Electrochemical performance of the TSC-200 and DSC-200. Reproduced with permission: Copyright 2024, American Chemical Society [71]. (c) SEM and TEM of FRA. (d) The water consumption, energy consumption, and greenhouse gas emission in producing 1 kg of different graphite anode materials. Reproduced with permission: Copyright 2022, Wiley-VCH GmbH [72].

### 3.1.1 | Lithium-Ion Battery (LIB)

As mainstream products of EES devices, LIBs have received widespread recognition due to their high energy capacity and stability [62]. However, huge challenges still exist for the upgradation of battery components to satisfy the constantly increased demand for energy [63–66]. The HTS technique has great potential in the field of exploitation of novel carbon-based materials for LIBs [67].

The graphite, as the anode material, still shows deficiency in diffusion kinetics and interfacial reaction kinetics in the field of fast-charging appliances [68–70]. Huang et al. thermodynamically facilitated graphitization with a thermal shock at an ultrahigh temperature (3228 K) and prepared hybrid-structured carbon composed of crystalline and amorphous carbon under a mechanical shock (Figure 6a) [71]. It demonstrates a great capacity (Figure 6b). With the increasing use of batteries, the mishandling of disposed carbon anode will result in severe environmental impacts. Hence, recycling them is a prospective option. Chen et al. [72] regenerated the graphite anode applying HTS to efficiently remove the organic binder at the graphite anode and decompose the resistive impurities like solid-electrolyte interface, while preserving the graphite structure from being damaged at the same time (Figure 6c,d).

The capacity of graphite still has limitations. Chen et al. introduced a rapid thermal shock process utilizing HTS to

create a conductive RGO composite embedded with silicon nanoparticles (Figure 7a) [73]. The embedding of silicon facilitates electron transfer (Figure 7b). Liu et al. prepared ultra-small silicon nanoparticles (us-Si/C) by FJH technology [74]. These particles were uniformly embedded in the carbonized nanosheets (Figure 7c). This unique structural design not only displays high-discharge activity of ultrafine Si nanoparticles but also buffers the damage from the volume change of Si up to 400% (Figure 7d). Its utility was further confirmed in the  $\text{LiFePO}_4$  cathode-constructed full cell. Meanwhile, Yang et al. [75] controlled the thermal interaction between carbon and silicon phases, effectively minimizing phase segregation issues in conventional heat treatment (Figure 7e). Additionally, the construction of core-shell structure provides another accessible strategy to mitigate the phase segregation problem. To alleviate internal stress release and contact between the Si/C composites during lithiation, Liu et al. reported a type of SS-Si/C composite (Figure 7f) [76]. The obtained Si/C composites are demonstrated in the construction of high energy density, long cycling life LIBs (Figure 7g) [77].

Metallic Li anodes face two main challenges, which are dendritic growth and unstable interface (Figure 8a) [78]. Yang et al. prepared uniform silver (Ag) nanoparticles (~40 nm) on CNF by HTS technique, which can effectively modulate the deposition behavior of Li, leading to a uniform dispersion of Li within the 3D carbon architecture (Figure 8b) [79]. Shan et al. successfully synthesized vertical graphite (VG) modified nickel sulfides



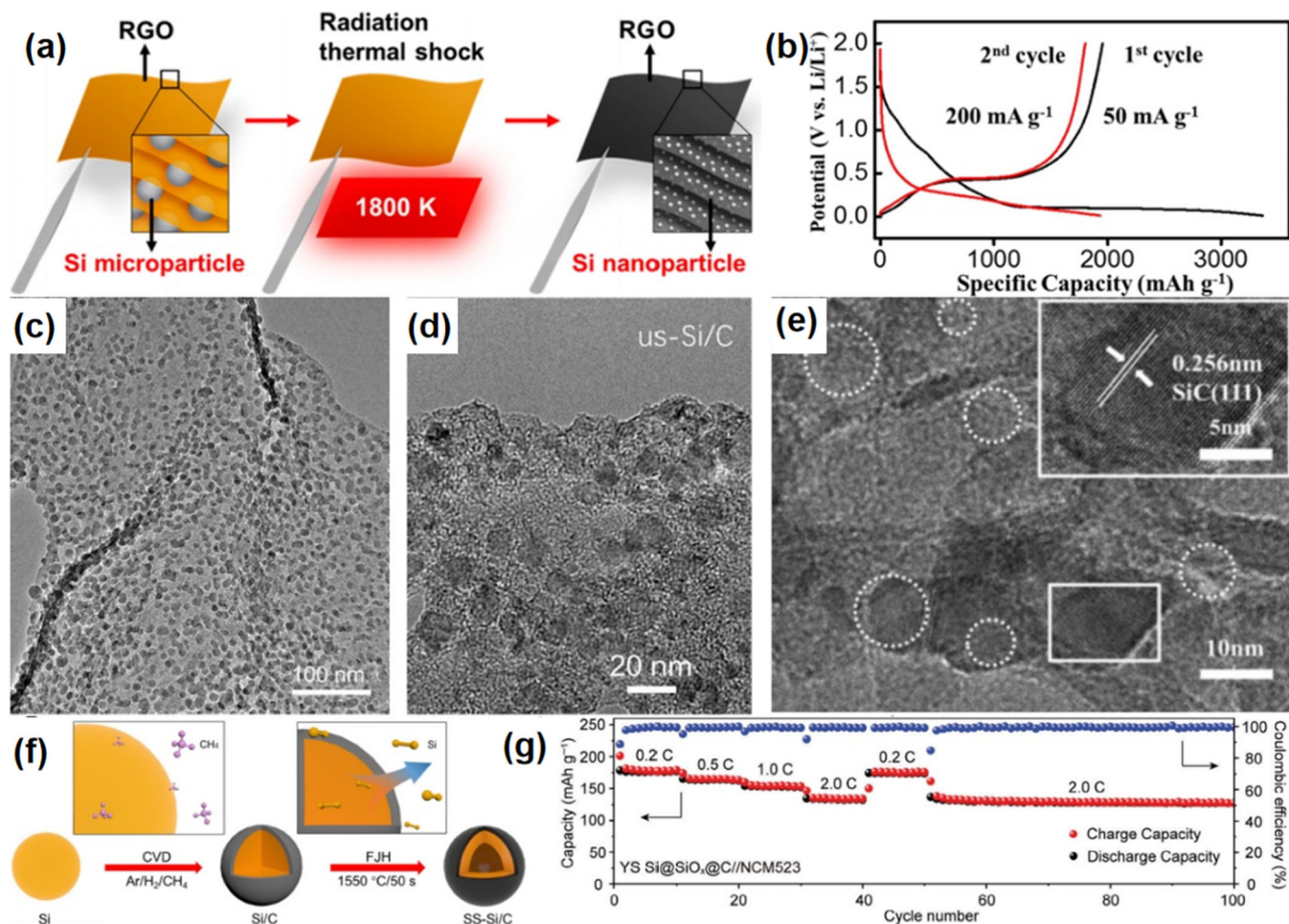


**FIGURE 7** | (a) Schematic illustration of the synthesis of RGO-SiNPs from RGO-SiMPs. (b) Performance diagram of RGO SiNP thin film. Reproduced with permission: Copyright 2016, American Chemical Society [73]. (c, d) TEM images of us-Si/C electrodes (c) before the cycle and (d) after 200 cycles. Reproduced with permission: Copyright 2024, Royal Society of Chemistry [74]. (e) HRTEM image of F-Si@rGO. Reproduced with permission: Copyright 2024, Elsevier [75]. (f) Schematic illustration of the synthesis process of SS-Si/C. Reproduced with permission: Copyright 2024, American Chemical Society [76]. (g) Rate capability of the material. Reproduced with permission: Copyright 2024, Wiley-VCH GmbH [77].

(Ni<sub>3</sub>S<sub>2</sub>) nanoparticles on carbon cloth (CC) substrate by HTS technique (Figure 8c) [80]. SEM and TEM characterization results demonstrate uniformly distributed Ni<sub>3</sub>S<sub>2</sub> nanoparticles with diameters ranging from 5 to 30 nm on VG nanofilms (Figure 8d,e). Even under high current density, for over 50 dynamic lithium deposition and stripping cycles, the surface of CC/VG@Ni<sub>3</sub>S<sub>2</sub>-Li electrode remains smooth, demonstrating significantly suppressed lithium dendritic growth (Figure 8f).

HTS technique offers solutions to various problems faced by conventional synthesis methods in preparation of other components of LIBs, including complicated reactions and high risks of failure [81, 82]. Take the current collector as an example, lightweight, highly conductive candidates such as RGO films show great potential in replacing traditional metal current collectors. However, their relatively low conductivities and high costs challenge them to meet the requirements for practical battery manufacturing. Therefore, it is crucial to resolve these problems of carbon-based films to fabricate flexible, lightweight, highly conductive, and affordable current collectors for lithium batteries. In this attempt, Chen et al. prepared RGO film with excellent electrical conductivity

through HTS [83]. The defects in adjacent RGO layers promote cross-linking, which drives a sharp increase in the conductivity of RGO films after high-temperature annealing.

### 3.1.2 | Li-S/Li-O<sub>2</sub> Batteries (LSB)

LSBs exhibit significant promise as next-generation energy storage solutions, owing to their high theoretical energy density and cost-effectiveness [84, 85]. However, the slow redox kinetics of sulfur species and the shuttle effect of lithium polysulfides (LiPSs) lead to underwhelming utilization of sulfur species and limited cycling life [86]. Therefore, it is crucial to develop advanced materials with sulfur anchoring and catalysis abilities for improving the electrochemical performance of LSBs [87].

Carbon-based nanomaterials synthesized by HTS technique can act as catalysts for Li-S species. Xu et al. successfully designed and prepared CoNiFePdV high entropy alloy (HEA) nanocatalysts via HTS technique (Figure 9a) [88]. The incorporation of five elements (Co, Ni, Fe, Pd, and V)

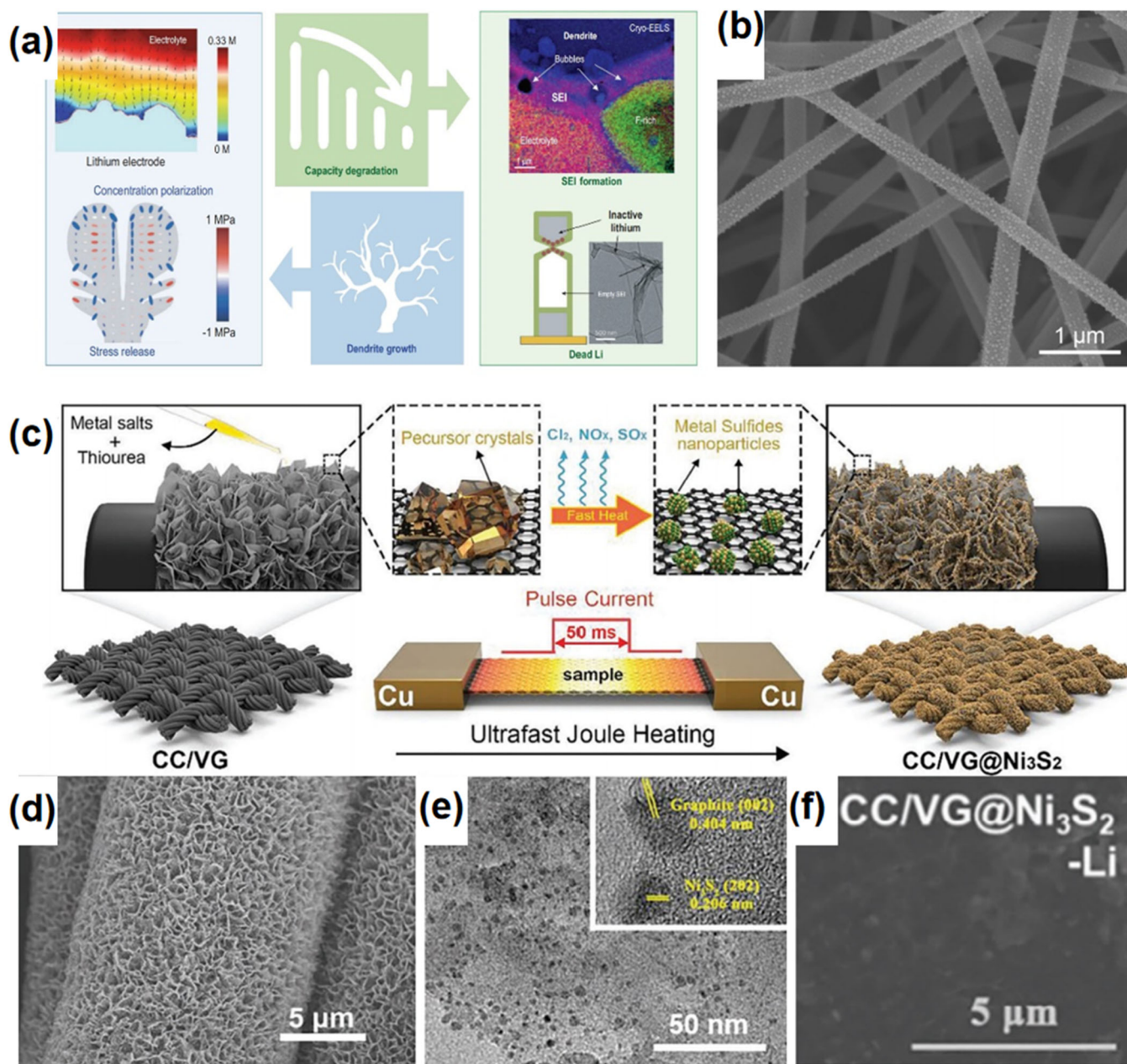


**FIGURE 8** | (a) Four factors affecting the cycling life of rechargeable lithium-metal batteries. Reproduced with permission: Copyright 2022, Oxford University Press [78]. (b) SEM images of AgNPs on CNFs synthesized via HTS. Reproduced with permission: Copyright 2017, Wiley-VCH GmbH [79]. (c) Scheme illustration of the CC/VG@Ni<sub>3</sub>S<sub>2</sub> synthesis process. (d) SEM, (e) TEM and HRTEM images of CC/VG@Ni<sub>3</sub>S<sub>2</sub> scaffold. (f) SEM images of disassembled symmetric cells fabricated with CC/VG@Ni<sub>3</sub>S<sub>2</sub> after 50 cycles. Reproduced with permission: Copyright 2024, Wiley-VCH GmbH [80].

into a single HEA greatly accelerates the multi-electron and stepwise sulfur redox reactions. Wang et al. synthesized a heterostructured WO<sub>x</sub>/W<sub>2</sub>C nanocatalyst via ultrafast Joule heating, and the resulting heterointerfaces enhance the electrocatalytic activity for Li<sub>2</sub>S oxidation while promoting controlled Li<sub>2</sub>S deposition (Figure 9b) [89]. An internal electric field was established at the interface of the heterostructure by Dong's team [90]. This field enhanced the mobility of electrons and ions, thereby facilitating the sulfur reduction reaction (SRR). These findings contribute to a deeper understanding of the rapid redox kinetics of sulfur species, laying a theoretical foundation for the advancement of high-performance Li-S batteries.

Li-O<sub>2</sub> batteries with ultrahigh energy density (~3500 Wh kg<sup>-1</sup>) are another prospective candidate for high-performance electrochemical devices, and they attracted extensive research interests [92]. Jung et al. prepared quaternary combinations of four elements (Pt, Pd, Au, and Ru) nanoparticles (NPs) [91]. The PtPdAuRu/CNF cathode demonstrated a significantly lower overpotential of 0.45 V (Figure 9e). It can be ascribed to the improved catalytic activity stemming from a greater affinity for O<sub>2</sub> in the quaternary nanoparticles. Lastly, HTS technique also exhibits superior versatility in preparation of electrodes for Zinc-air batteries [93, 94], and Lithium-carbon dioxide batteries [95, 96].



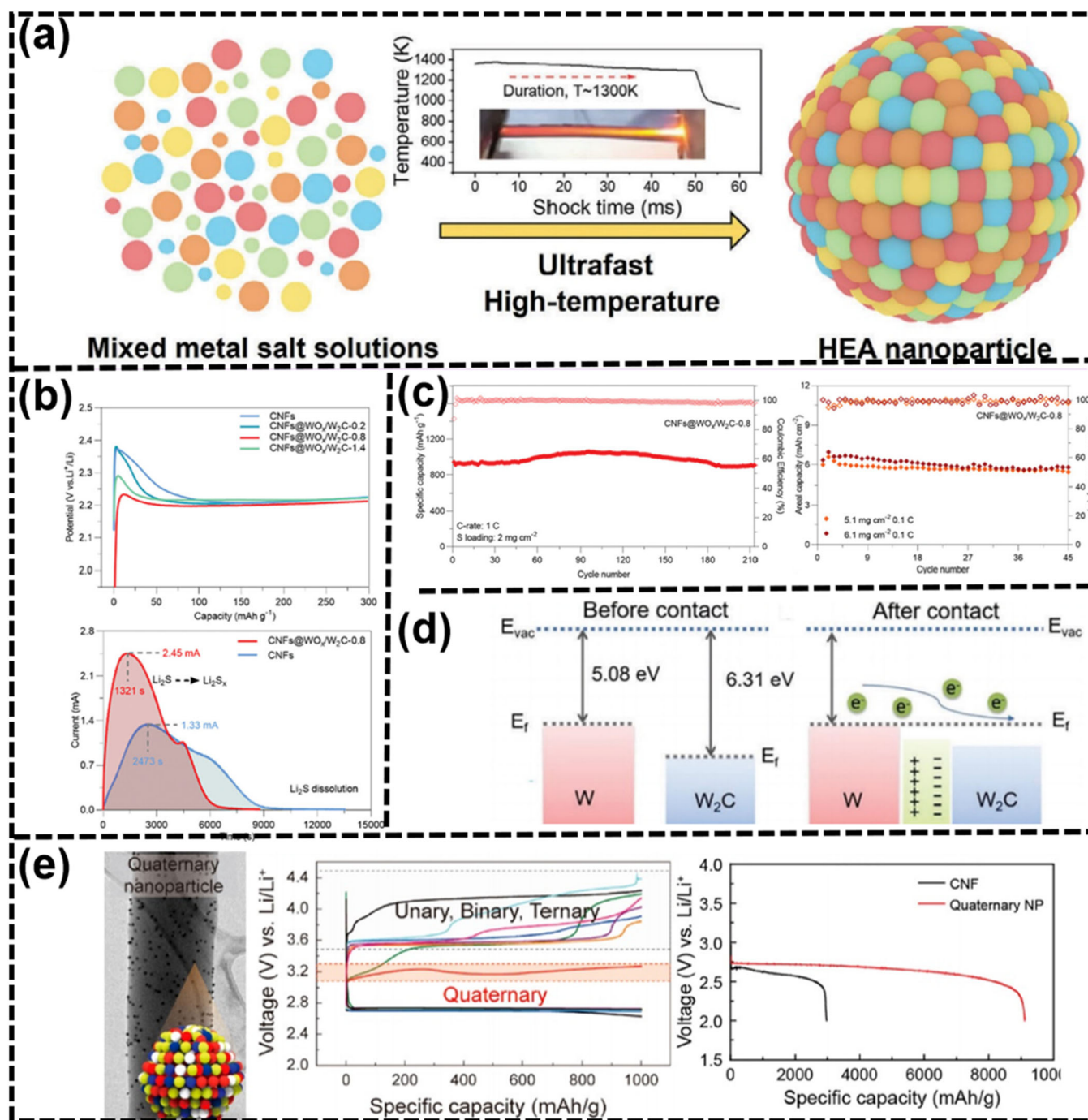


**FIGURE 9** | (a) Formation and structural characterization of CoNiFePdV high-entropy alloys. Reproduced under terms of the CC-BY license [88]. Copyright 2024, Yunhan Xu, Wenchuang Yuan, Chuannan Geng, et al., published by Wiley-VCH GmbH. (b,c) The performance diagram of CNFs@WO<sub>x</sub>/W<sub>2</sub>C-0.8. Reproduced with permission: Copyright 2024, Wiley-VCH GmbH [89]. (d) Schematic diagrams of band structures for W and W<sub>2</sub>C before and after their contact. Reproduced under terms of the CC-BY license [90]. Copyright 2024, Huiyi Dong, Lu Wang, Yi Cheng, et al., published by Wiley-VCH GmbH. (e) Performance of the electrodes. Reproduced with permission: Copyright 2021, American Chemical Society [91].

In summary, in the field of EES, HTS technique has shown remarkable potential. The ultrahigh processing temperature and ultra-fast heating and cooling rates of HTS facilitate the construction of highly stable electrodes. Based on current research, the construction of carbon-based material electrodes without metal collector nor chemical binders by HTS technique is a feasible strategy for the development of high-energy density batteries.

## 3.2 | Electrochemical Catalysis

### 3.2.1 | Electrocatalytic Water Splitting

Hydrogen production via water electrolysis represents a widely investigated and pursued green energy technique, generating a pristine, eco-friendly, and renewable energy source by cleaving water molecules into hydrogen and oxygen. This process



necessitates the utilization of catalysts to facilitate water splitting and hydrogen production. Carbon-based nanomaterials have been widely utilized in catalyzing the HER and OER. Different carbon structures produced through HTS, significantly influence the efficiency of HER and OER [97]. Nanosized transition metal carbides with hexagonal crystal symmetry have emerged as excellent catalysts for the HER process due to their platinum-like electronic structure [98]. The Mo<sub>2</sub>C synthesized by the Joule heating has a unique surface structure, a larger specific surface area, and is directly anchored on carbon black during HTS synthesis. The Zong team reported an innovative method for the rapid synthesis of Mo<sub>2</sub>C-based electrocatalysts through Joule heating. This newly synthesized catalyst demonstrated enhanced HER performance compared to commercially available Mo<sub>2</sub>C [99].

Carbon-based nanomaterials can be prepared rapidly by HTS method, and the structure of the nanomaterials may deviate significantly from thermodynamic equilibrium, forming metastable materials. The metastable phase may significantly influence interactions with essential reaction intermediates, thereby affecting the resulting electrocatalytic activity [54]. The Joule heating method offers remarkable advantages in rapidly synthesizing metastable materials and regulating metastable phases by adjusting synthetic parameters. Liu's team synthesized high-efficiency Mo<sub>2</sub>C/MoC/CNT hydrogen evolution reaction catalysts by tuning the reaction duration, demonstrating that the ratio of MoC (111) to Mo<sub>2</sub>C (002) decreases with increased heating time (Figure 10a) [101]. The research confirms the gradual transformation of MoC to Mo<sub>2</sub>C under elevated temperatures. It is essential to synthesize the Mo<sub>2</sub>C/MoC heterostructure within a short timeframe to optimize electrocatalytic performance. Many Mo<sub>2</sub>C/MoC heterointerfaces provide sufficient active sites for high HER performance. Additionally, Xiong's team prepared tungsten carbide electrodes with different Joule heating durations (3, 10, 30, and 60 s) to fine-tune the phase composition of the tungsten monocarbide (WC) and tungsten semicarbide (W<sub>2</sub>C) mixture [103]. Electrocatalytic evaluations indicate that samples subjected to a 30-s treatment period demonstrate an optimal phase composition, resulting in a low overpotential. Deng's team selectively synthesized phase-pure molybdenum carbides by adjusting pulse voltages during the HTS synthesis (Figure 10b) [53]. The study reveals the phase-dependent performance of molybdenum carbides in HER. Owing to the kinetically controlled ultrafast cooling, Joule heating can be easily extended to the phase engineering of metastable carbides, which has been demonstrated to be effective in improving the carbides' electrocatalytic performance.

Heteroatom-doped carbon materials are a specialized group of carbon-based substances that incorporate small quantities of heteroatoms into their carbon framework. Specifically, non-metal heteroatoms such as N, S, P, B, and halogens can induce various beneficial effects when integrated into the structure [104, 105]. Heteroatom-doped carbon materials have emerged as innovative and highly effective electrocatalysts. They not only maintain excellent electrical conductivity but also provide abundant active sites [106]. The Joule heating synthesis distinguishes itself from conventional posttreatment doping methods by eliminating the need for excessive gas or liquid phase heteroatom sources, additional catalysts, prolonged

reaction time, and cumbersome purification procedures. In a typical Joule heating process, the rapid rise in temperature causes the volatilization of heteroatom components, thereby facilitating homogeneous reactions between precursor vapors and the carbon source. This interaction ultimately results in the formation of doped carbon materials [107]. The Li team demonstrated the synthesis of fine CoNi nanoparticles by HTS, measuring 5–6 nm, which are supported within a network of nitrogen-doped defective CNTs. The presence of nitrogen-doped sites alters the local symmetry and electronic structure, enabling these sites to function as active centers for a range of electrocatalytic processes. Heteroatom doping alters the local symmetry and electronic properties of carbon materials, enhancing their electrocatalytic performance by creating active sites [108]. Zhu's team utilized FJH to rapidly synthesize carbon-supported high-entropy alloy sulfide nanoparticles (CC-S-HEA) on carbon cloth within just 300 ms, achieving strong self-standing properties [102]. The thermal shock produced by HTS can pyrolyze the sulfur source into gaseous form, leading to the formation of diverse pore structures and defects in the carbon material (CC). This process creates a sulfur-doped carbon substrate (CC-S) (Figure 10c). Subsequently, sulfur atoms anchor metal atoms onto the CC-S surface. The high density and uniform distribution of metal particles create high electrochemical performance.

Carbon-based materials are renowned for their exceptional electron transfer properties and resistance to corrosion, making them ideal substrates for the development of metal nanoparticle electrocatalysts. An effective approach to enhancing electrocatalyst efficiency involves developing carbon-supported nanocrystals that feature abundant active sites. However, ultrafine nanoparticles tend to agglomerate into larger particles over extended operational periods and may dissolve in harsh acidic environments. A promising solution is to anchor these ultrafine nanoparticles onto a carbon matrix using Joule heating, which can significantly mitigate both agglomeration and dissolution issues [109]. The strong interaction between metal and support can significantly enhance both the activity and stability of catalysts by preventing nanoparticle agglomeration and increasing the affinity between nanoparticles and supports. Zong's team successfully synthesized NiRu alloy nanoparticles that are well-dispersed on nitrogen-rich CNTs (NiRu-CNTs) using a FJH method that completed in just 0.5 s (Figure 10d) [100]. The NiRu-CNTs demonstrate exceptional HER and OER performance (Figure 10e). It is crucial to anchor alloys securely onto carbon supports to enhance the performance of HER and OER activities. The Joule heating technique, known for its rapid heating and cooling capabilities, has been identified as an effective approach for loading nanoparticles onto carbon supports, ensuring a strong metal-support interaction.

The Joule-heating method enables the rapid synthesis of a wide range of carbon and carbon-based nanomaterials, which demonstrate exceptional activity and stability in electrocatalytic HER and OER. This efficient synthesis approach not only significantly shortens the preparation time but also plays a crucial role in enhancing water-splitting efficiency. Consequently, it offers promising opportunities for advancing sustainable technologies for hydrogen and oxygen production.

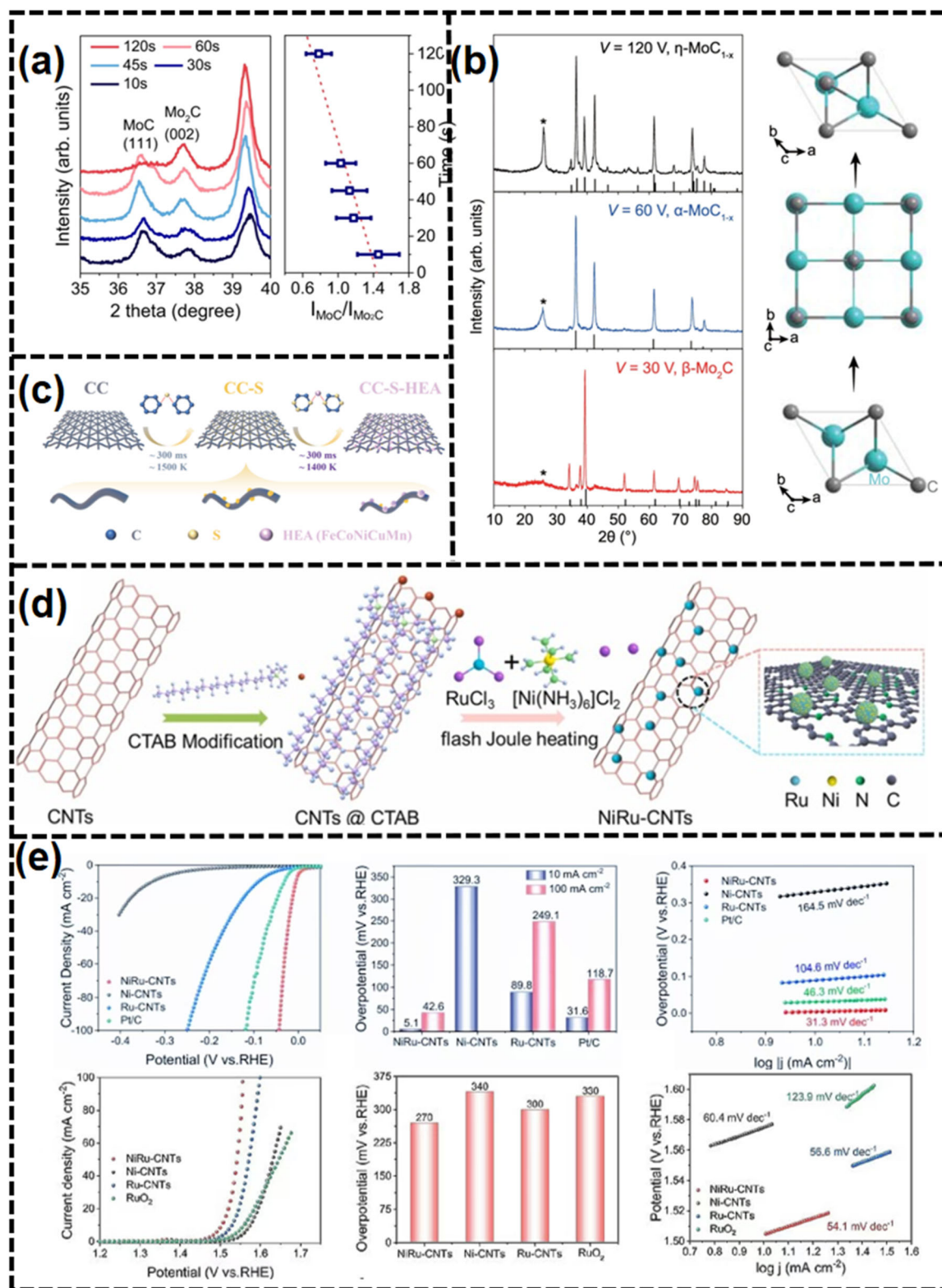


**FIGURE 10** | (a) XRD of  $\text{Mo}_2\text{C}$ /MoC/CNT. Reproduced under terms of the CC-BY license [101]. Copyright 2022, Chengyu Li et al, published by Springer Nature. (b) XRD and structural diagrams of  $\beta\text{-Mo}_2\text{C}$ ,  $\alpha\text{-MoC}_{1-x}$ , and  $\eta\text{-MoC}_{1-x}$ . Reproduced under terms of the CC-BY license [53]. Copyright 2022, Bing Deng et al, published by Springer Nature. (c) Schematic diagram of the synthesis mechanism of CC-S-HEA. Reproduced with permission: Copyright 2023, Tsinghua University Press [102]. (d) Schematic illustration of the synthesis process of NiRu-CNTs catalyst. (e) Electrochemical performance diagrams of the materials. Reproduced with permission: Copyright 2023, Elsevier [100].

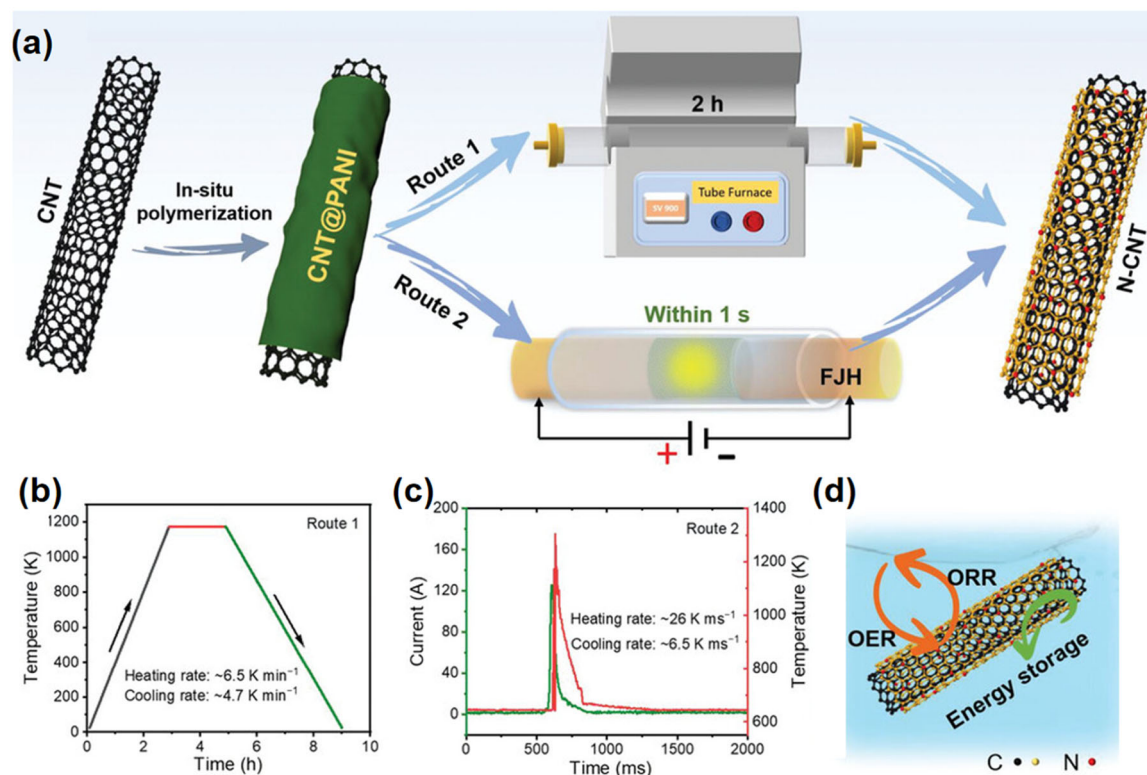


**FIGURE 11** | (a) A schematic representation comparing the traditional and FJH synthesis methods for N-CNTs. (b) The temperature profile associated with conventional synthesis processes. (c) The temperature profile corresponding to the FJH synthesis method. (d) The electrochemical performance metrics of the synthesized N-CNTs in relation to energy storage and conversion applications. Reproduced with permission: Copyright 2024, Wiley [112].

### 3.2.2 | Electrocatalytic Oxygen Reduction Reaction (ORR)

The electrocatalytic ORR is pivotal for energy conversion processes. However, the sluggish kinetics and significant overpotential linked to the four-electron transfer mechanism hinder ORR efficiency. Consequently, there is a pressing need to identify effective, affordable, and stable catalysts, particularly carbon-based nanomaterials, as alternatives to precious metal catalysts like platinum. Traditional synthesis methods for these materials often require considerable time. In contrast, the FJH method presents new opportunities, enabling rapid heating, achieving higher temperatures (up to 3000 K), and facilitating swift heating and cooling compared to conventional techniques.

Research has extensively demonstrated that graphitic-N enhances electron transport and acts as a catalytic site in various reactions [110]. However, conventional methods often encounter challenges, including complex processing procedures, extended reaction times, specific atmospheric requirements, and high costs. These factors pose significant obstacles to large-scale production [111]. The FJH technology offers notable advantages in the synthesis and modification of carbon materials, characterized by its exceptionally short synthesis time and minimal energy consumption. The Zhu team successfully created a metal-free heteroatom-doped carbon material (N-CNT) using the efficient FJH method, achieving results in just 1 s (Figure 11) [112]. The flash N-CNTs demonstrate remarkable catalytic activity for the ORR. This performance is comparable

to that of samples produced via the traditional, labor-intensive pyrolysis method.

FJH method facilitates almost instantaneous turnarounds between rapid heating and rapid cooling of the reaction zone, by simply turning on and off the electrical field. It is thus favorable for producing uniform-sized, fine nanoparticles by suppressing their further aggregation or agglomeration that often occurs in traditional thermal processes due to prolonged annealing at high temperatures. The carbon substrate not only prevents nanoparticles from aggregation but also promotes electron transport for their electrocatalytic operations. Yang team produced carbon-supported Pd-Se nanoparticles by quick Joule heating (Figure 12) [113]. The fine nanoparticle size and their uniform distribution on the carbon substrate led to excellent ORR performance in an alkaline medium. The carbon-supported cubic  $\text{Pd}_{17}\text{Se}_{15}$  nanoparticles exhibit a higher half-wave potential (0.89 V) relative to commercial Pd/C catalyst (0.85 V) in an alkaline solution. This demonstrated the potential of carbon-supported nanoparticles in developing highly efficient electrocatalysts for ORR.

### 3.2.3 | Electrocatalytic Carbon Dioxide Reduction Reaction ( $\text{CO}_2\text{RR}$ )

Wulan et al. heated  $\text{In}(\text{OH})_3$  precursors up to  $800^\circ\text{C}$ – $2400^\circ\text{C}$  using Joule heating to obtain the  $\text{In}/\text{In}_2\text{O}_3$  heterostructure (Figure 13a–e) [114]. The Joule heating process and in-situ



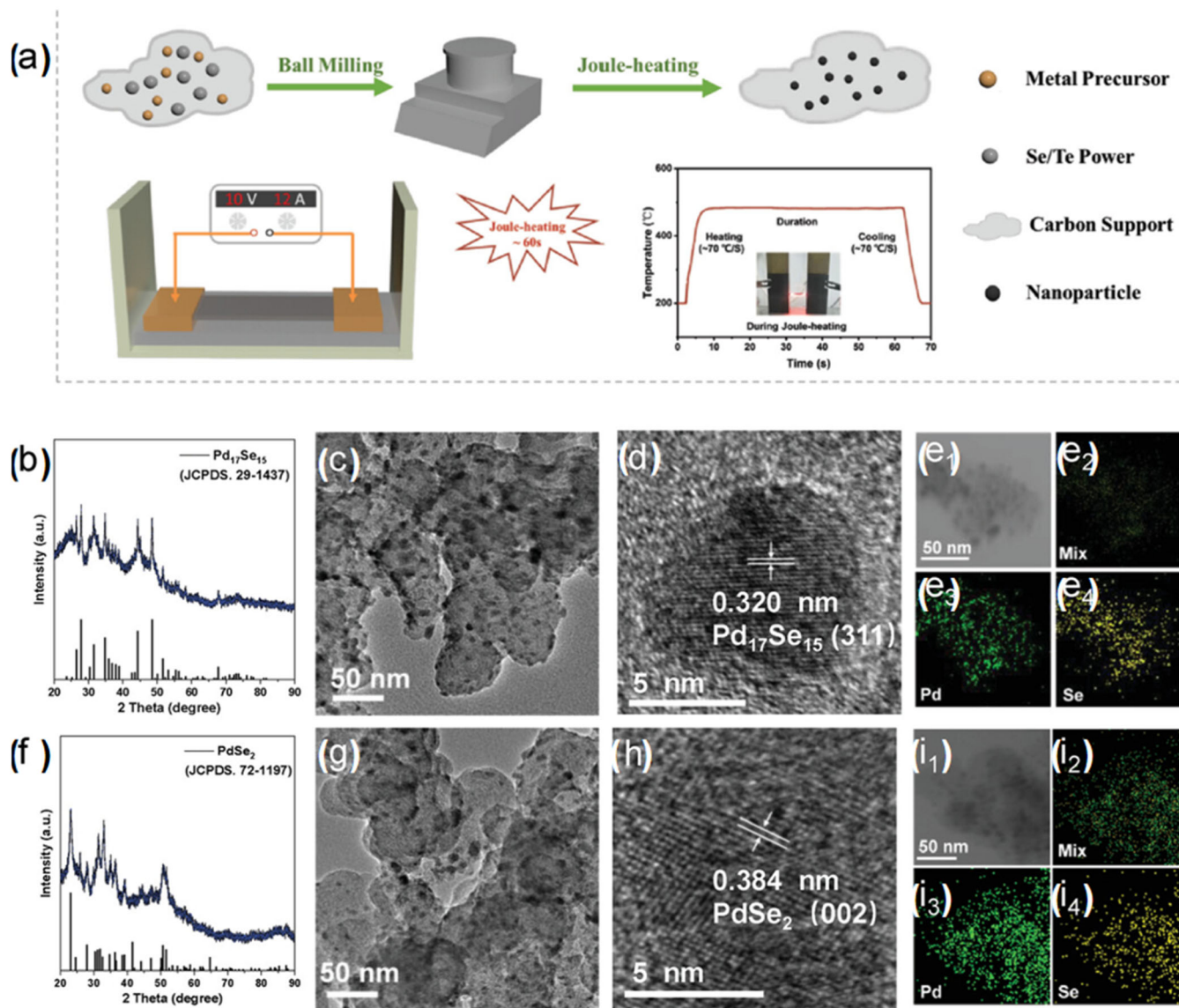


**FIGURE 12** | (a) The study presents a schematic representation. (b, f) XRD patterns, (c, g) TEM images, (d, h) HRTEM images, (e1, i1) scanning TEM images, and (e2–e4, i2–i4) corresponding element maps of the (b–e4)  $\text{Pd}_{17}\text{Se}_{15}$  NPs/C and (f–i4)  $\text{PdSe}_2$  NPs/C, respectively. Reproduced with permission: Copyright 2024, Wiley-VCH GmbH [113].

electrochemical reduction allowed precise engineering of the catalyst structure and surface properties, leading to the creation of heterogeneous interfaces. The optimized  $\text{In}/\text{In}_2\text{O}_3$  catalysts demonstrated improved performance in the electrocatalytic reduction of  $\text{CO}_2$ . The presence of  $\text{InO}$  species at hetero-interfaces effectively modulates surface chemistry, facilitates  $\text{CO}_2$  activation, and promotes efficient electrocatalytic conversion. This study highlights Joule heating as a new strategy to prepare novel catalysts for enhanced electrocatalytic performance.

However, the manufacturing cost of conventional  $\text{CO}_2$  reduction catalysts such as indium-based catalysts is high. Wang et al. successfully synthesized bismuth-containing nanoparticles (BI-NPS/FG) with carbon black and  $\text{Bi}(\text{NO}_3)_3 \cdot 5\text{H}_2\text{O}$  precursors in 200 ms using an ultra-fast and environmentally friendly FJH method [115]. The resulting Bi-NPs/FG hybrid demonstrated exceptional selectivity for  $\text{CO}_2$  electroreduction. This work

proposed a fast, scalable method for producing highly efficient electrocatalysts for  $\text{CO}_2$  conversion and other applications, highlighting the versatility and potential of the FJH method.

Nevertheless, monometallic catalysts always have their limitations. Therefore, researchers have turned their attention to high-entropy alloy systems composed of multiple metal elements [116]. Ahn et al. proposed a simple and effective method for the synthesis of HEA nanoparticle (HEA-NP) catalyst by carbon thermal shock (CTS) (Figure 13f,g) [52]. An amorphous  $\text{TiO}_2$  layer over the CNF substrate was produced by hydrolysis of TTIP precursor, and it was transformed into conformal crystalline layer by a medium power rapid thermal shock. The obtained  $\text{CNF@TiO}_2$  was subsequently immersed in mixed metal precursor solution ( $\text{RuRhPdIrPt}$ ) and dried, where the  $\text{TiO}_2$  layer enhanced the absorption of precursor ions. Well-dispersed and ultra-stable HEA-NPs anchored on carbon substrates were obtained via another rapid joule heating, which

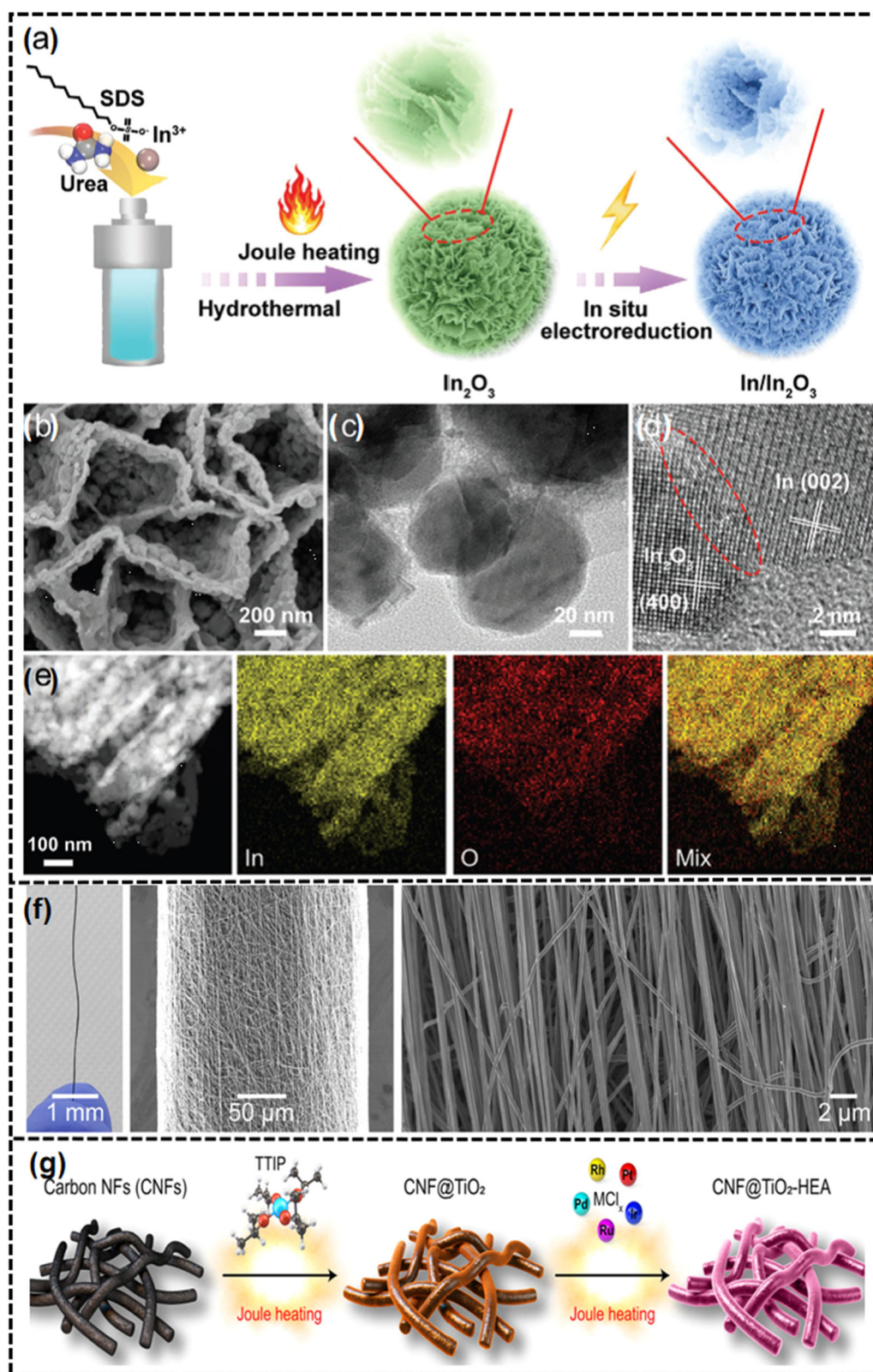


**FIGURE 13** | (a) Schematic illustration for preparation of the In/In<sub>2</sub>O<sub>3</sub> catalysts. (b) SEM, (c) TEM, (d) HRTEM images, and (e) the corresponding element mappings of In/In<sub>2</sub>O<sub>3</sub>. Reproduced with permission: Copyright 2024, Wiley-VCH GmbH [114]. (f) The photo and SEM images of CNF yarn. (g) Schematic illustration describing the synthetic protocol developed. Reproduced with permission: Copyright 2023, American Chemical Society [52].

resulted in the thermal degradation of precursors into the alloy. The strong interaction between these metallic atoms and the oxide surface effectively slowed down their diffusion and attenuated particle agglomeration, resulting in high-density,

ultrasmall HEA-NPs smaller than 3 nm. Thermal shock led to the formation of a nested structure on the oxide surface, thereby preventing severe particle aggregation. As a model system, CNF@TiO<sub>2</sub>-HEA exhibited efficient thermal catalysis for



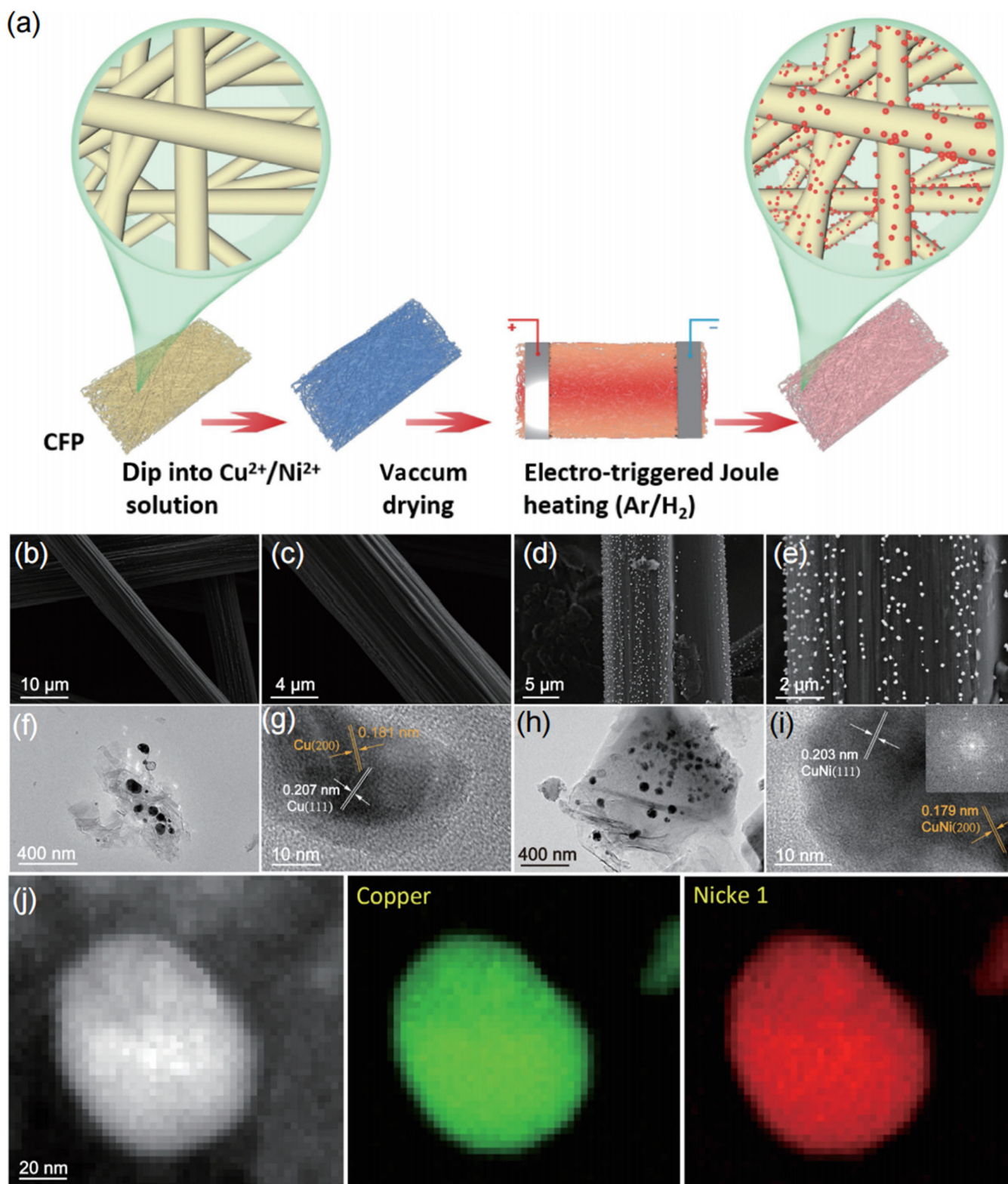


**FIGURE 14** | (a) Schematic illustration for CFP-Cu<sub>x</sub>Ni<sub>y</sub> synthesis. (b, c) SEM images of CFP. (d, e) SEM images of CFP-Cu<sub>1</sub>Ni<sub>1</sub>. (f, g) TEM and HRTEM images of CFP-Cu. (h, i) TEM and HRTEM images of CFP-Cu<sub>1</sub>Ni<sub>1</sub>. (j) EELS element mappings of CFP-Cu<sub>1</sub>Ni<sub>1</sub>. Reproduced with permission: Copyright 2023, Tsinghua University Press [118].

converting CO<sub>2</sub> to CO with a conversion of > 50%, a selectivity of > 99%, and a stable performance for over 300 h with minimal degradation. This work was an important contribution to the practical design of multiphase catalysts based on multi-element synergy.

Lastly, Joule heating also serves as an effective strategy for preparing carbon-supported single-atom catalysts (SACs) with minimized requirement of nitrogen dopants. Xi et al. prepared C<sub>250</sub>Ph<sub>3.5</sub> Ni SAC by heating the modified carbon black precursor at 1300°C by HTS, and the catalyst was used in CO<sub>2</sub>RR for a



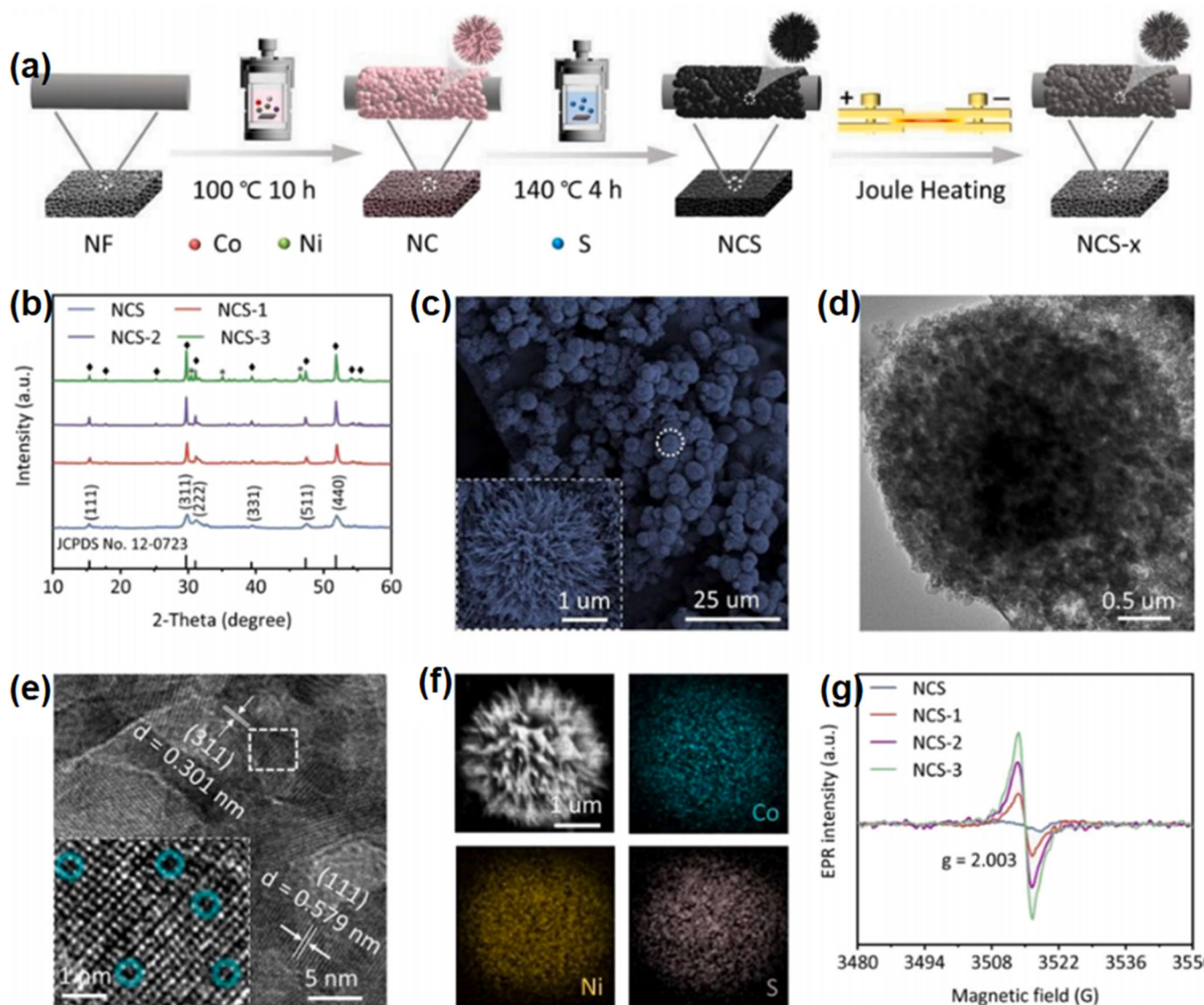


**FIGURE 15** | (a) Schematic illustration for NCS-x preparation. (b) XRD patterns for NCS and NCS-x. (c) SEM, (d) TEM, (e) HRTEM images of NCS-2, and (f) corresponding EDS elemental mappings. Insets: enlarged SEM and HRTEM images of highlighted regions. (g) EPR spectra of NCS and NCS-x. Reproduced with permission: Copyright 2023, Elsevier [119].

proof-of-concept [117]. It has been demonstrated that different types of nitrogen-doping, including graphitic, pyrrolic, and pyridinic nitrogen, considerably affect the performance of obtained SACs. Specifically, the absence of unfavorable nitrogen species in Ni SACs promotes  $\text{CO}_2\text{RR}$  reaction. Moreover, the remaining nitrogen dopants after the Joule heating are primarily coordinated with Ni, enhancing the catalyst's thermodynamic stability and electrocatalytic performance. This versatile Joule heating method has also been successfully extended to synthesize carbon-supported Fe, Co, Cu, and Zn SACs, highlighting its potential for various catalytic applications.

### 3.2.4 | Electrocatalytic Nitrate Reduction Reaction ( $\text{NO}_3\text{RR}$ )

Joule heating technology is also used in the preparation of electrocatalysts for electrochemical  $\text{NO}_3\text{RR}$ . Zhang et al. synthesized a single-phase  $\text{Cu}_1\text{Ni}_1$  nanoalloy catalyst uniformly

dispersed on carbon fiber paper (CFP) using the FJH method (Figure 14) [118]. CFP- $\text{Cu}_1\text{Ni}_1$  showed high electrocatalytic activity. Theoretical calculations revealed that alloying Cu with Ni into a single phase upshifts the d-band center, enhancing  $\text{NO}_3^-$  adsorption while weakening  $\text{NH}_3$  adsorption. This work presents a novel approach for the rapid synthesis of uniformly dispersed single-phase nano-alloy catalysts using the FJH technique, aimed at enhancing  $\text{NO}_3\text{RR}$  for ammonia production.

Joule heating technology is also applicable in fine-tuning the atomic to microscopic structures of electrocatalysts, especially sulfur and oxygen vacancies that are crucial in certain  $\text{NO}_3\text{RR}$  catalysts. Tao et al. proposed using HTS to regulate surface sulfur vacancies (SV) on nickel cobalt sulfide (NCS) (Figure 15) [119]. In a typical synthesis, NCS loaded with nickel foam is placed on a HTS device and heated under vacuum at  $500^\circ\text{C}$ – $1000^\circ\text{C}$  to obtain NCS-x catalysts with different concentrations of SVs. The NCS-2 catalyst, with an optimized concentration of SVs, exhibited an outstanding  $\text{NO}_3\text{RR}$  performance. The increase in charge density of Co sites enhances

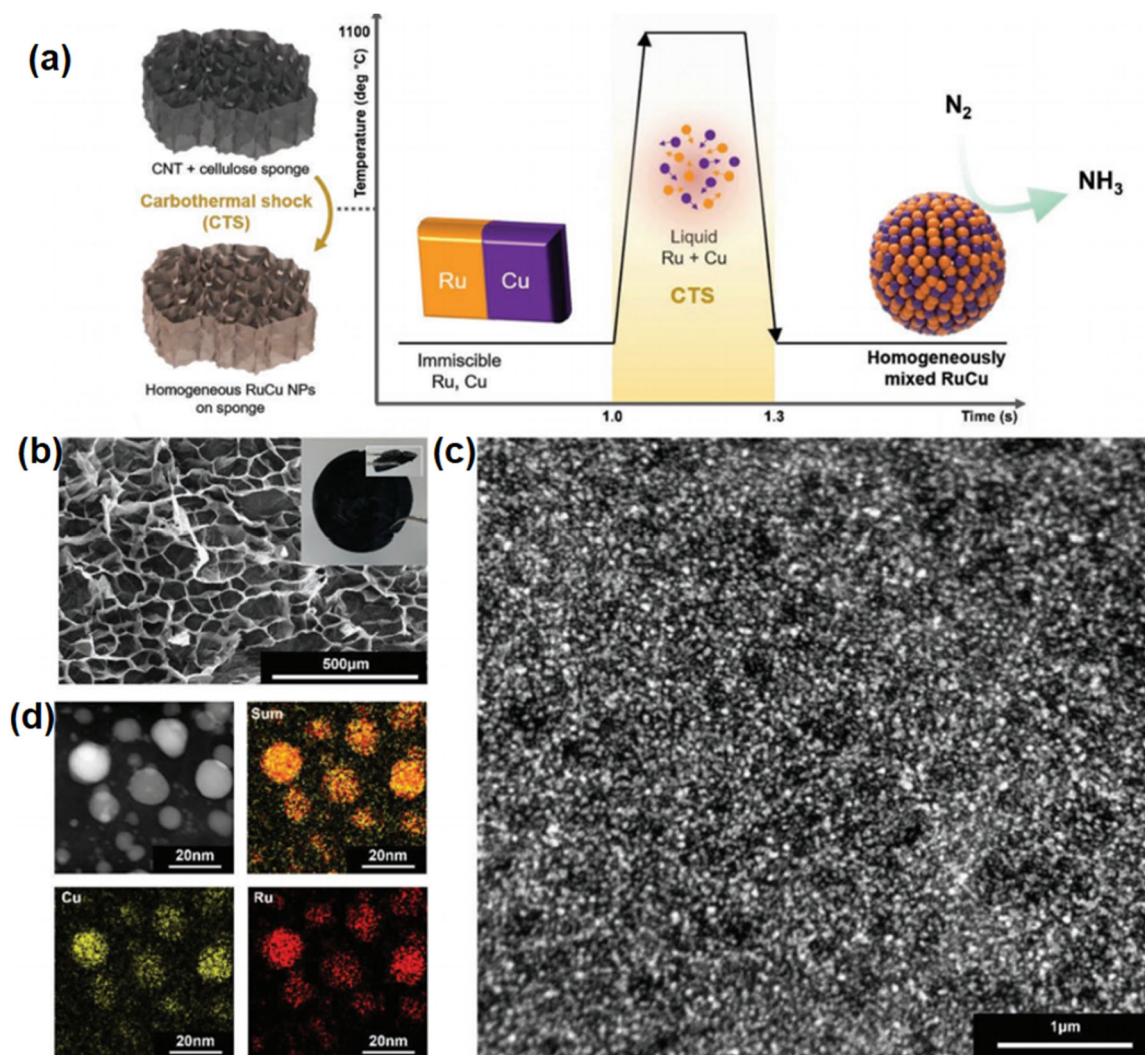


**FIGURE 16** | Morphology of atomic-scale homogeneous Ru–Cu NPs on cellulose/CNT sponge for NO<sub>3</sub>RR. (a) Schematic of the structure and fabrication of Ru–Cu NPs. (b) SEM images, (c) TEM dark field image, and (d) EDS elemental mappings of Ru–Cu NPs on the cellulose/CNT sponge. Reproduced with permission: Copyright 2022, Wiley-VCH GmbH [120].

the adsorption of NO<sub>2</sub>\* and reduces the free energy of the rate-determining step. This work provides a novel strategy for inducing SVs to enhance NO<sub>3</sub>RR activity, offering insights into simultaneous nitrate pollution reduction and electrocatalytic ammonia production.

In addition, Joule heating technology is also capable of preparing homogeneous mixtures of elements with large lattice structure differences that are otherwise immiscible. Kim et al. prepared well-mixed Ru–Cu nanoparticles (NPs) on cellulose/CNT sponges by a facile CTS synthesis (Figure 16) [120]. The Ru–Cu NPs exhibited remarkable NH<sub>3</sub> selectivity. This performance surpasses other reported Ru-based catalysts for electrochemical N<sub>2</sub> reduction reaction (NRR). The CTS method successfully facilitated the creation of a homogeneous alloy from the typically immiscible metals Ru and Cu, representing the first use of Ru–Cu NPs as electrocatalysts for NRR. The solid solution was found to enhance the NRR performance by favoring N<sub>2</sub> adsorption over hydrogen binding, leading to selective NRR on the catalyst surface. Additionally, the high density of NPs distributed on the cellulose/CNT sponge furnished

numerous active sites for enhanced ammonia production. This work offers valuable insights into preparation of solid solutions that are otherwise inaccessible by conventional synthesis for high-performance NRR via the CTS method.

### 3.2.5 | Other Electrocatalytic Reactions

In addition, the application of HTS-synthesized carbon-based nanomaterials in other electrocatalytic reactions, such as urea oxidation reaction (UOR), methanol oxidation reaction (MOR), ethanol oxidation reaction (EOR), glucose oxidation reaction (GOR), benzene series oxidation, ammonia oxidation reaction (AOR), and so on, is gradually expanding. Hu et al. presented a method that integrates rapid Joule heating with solid-phase synthesis to create carbon-loaded PdSe nanoparticles characterized by their small size, clean surfaces, and well-controlled crystal phases [113]. This approach not only demonstrates significant catalytic activity in the ORR but also exhibits impressive performance in the electrocatalysis of EOR. The introduction of Se into Pd alters its electronic characteristics,



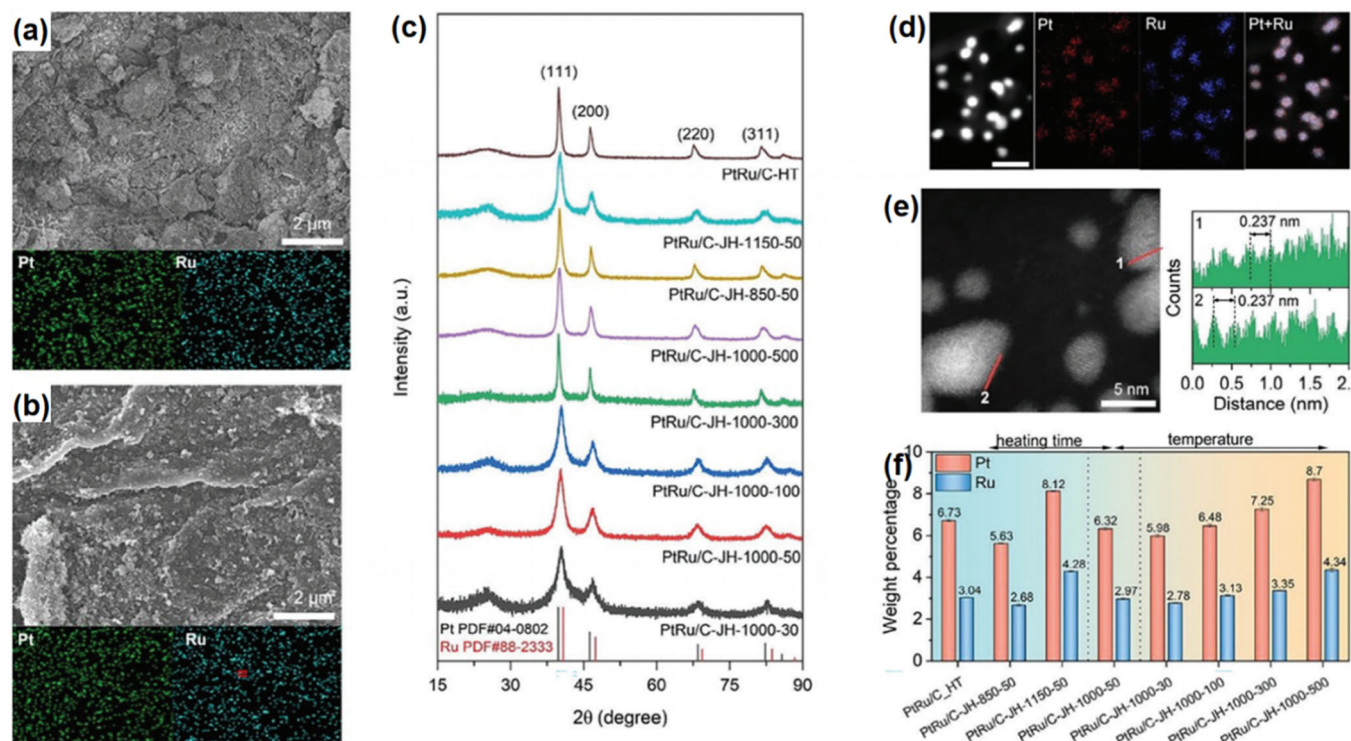


**FIGURE 17** | (a, b) SEM, EDX, XRD of PtRu/C-JH-1000-50. (c) XRD of PtRu/C. (d) HAADF-STEM and EDX mappings of PtRu/C-JH-1000-50. (e) HRTEM image of PtRu nanoparticles. (f) Mass fractions of Pt and Ru in PtRu/C. Reproduced with permission: Copyright 2024, Wiley [123].

which reduces the adsorption strength of critical reaction intermediates on Pd Se nanoparticles during the ORR and EOR processes. This modification enhances their electrocatalytic efficiency in these reactions. The versatility of this synthesis strategy for producing carbon-supported noble metal sulfide nanoparticles is underscored, highlighting its potential in the development of effective electrocatalysts.

However, as HTS is a new technology developed in the past decade, its research has not yet fully covered all electrocatalytic fields. Researchers are working hard to apply HTS-synthesized carbon-based nanomaterials in these fields.

### 3.2.6 | Electrocatalytic Energy Conversion Fuel Cells

Fuel cells hold significant promise as energy conversion devices for end users [121, 122]. This section describes the improvement of fuel cell materials using HTS technology. Carbon-supported metal nanoparticles prepared by conventional catalyst synthesis methods are challenged by the difficulty in precisely controlling their compositions and structures, and HTS technique offers the opportunity to further improve their electrocatalytic performance. Chen et al. report pioneering work on the fabrication of metal nanoparticles supported on carbon materials by ultrafast heating methods [73]. The Si/RGO hybrid film was subjected to heating through radiation emitted from a Joule-heated RGO film. This process led to the in situ conversion of larger Si particles into nanoparticles with dimensions ranging from 10 to 15 nm within 30 s at a temperature of 1800 K. Additionally, the technique was adapted to synthesizing nickel nanoparticles from micro-sized nickel particles. The resulting nickel/RGO

hybrid films were then utilized as catalysts in hydrogen peroxide fuel cells [123].

Deng et al. reported that direct Joule heating at optimized conditions of 1000°C over 50 ms led to the formation of homogeneous PtRu alloy nanoparticles on a carbon black substrate (Figure 17), with mass loadings determined to be 6.32 wt.% (Pt) and 2.97 wt.% (Ru) [124]. At similar mass loadings, the dimensions of PtRu alloy nanoparticles produced by the Joule heating method were much smaller than those produced by the standard hydrothermal method. High-temperature rapid heating can cause the metal precursor to fully decompose and not grow in time. The optimized PtRu/C-JH-1000-50 showed the highest mass activity. DFT calculations showed that Pt sites of the PtRu alloy nanoparticles have strong methanol adsorption capacity and weak CO binding ability, resulting in better MOR activity. A 24-h test in a two-electrode methanol fuel cell showed that the PtRu/C-JH-1000-50 also has decent stability, maintaining 85.3% of its initial current density. Characteristic XRD peaks of PtRu alloy nanoparticles were well maintained, suggesting minimal oxidation of Pt. These results recommended that the Joule heating method can prepare high-performance alloy nanoparticle catalysts for direct methanol fuel cell, where the fine-tuning of the nanoparticle structure through adjusting synthesis parameters is the key to optimized catalysts.

In another work, Julio et al. prepared a Pt electrocatalyst for the oxidation of the  $H_2 + CO$  mixture (Figure 18) [125]. There were structural defects in the synthesized Pt. The results highlight the enhanced CO tolerance of FJHM-Pt/C, which can be attributed to factors such as structural defects within the Pt and improved metal-support interactions.



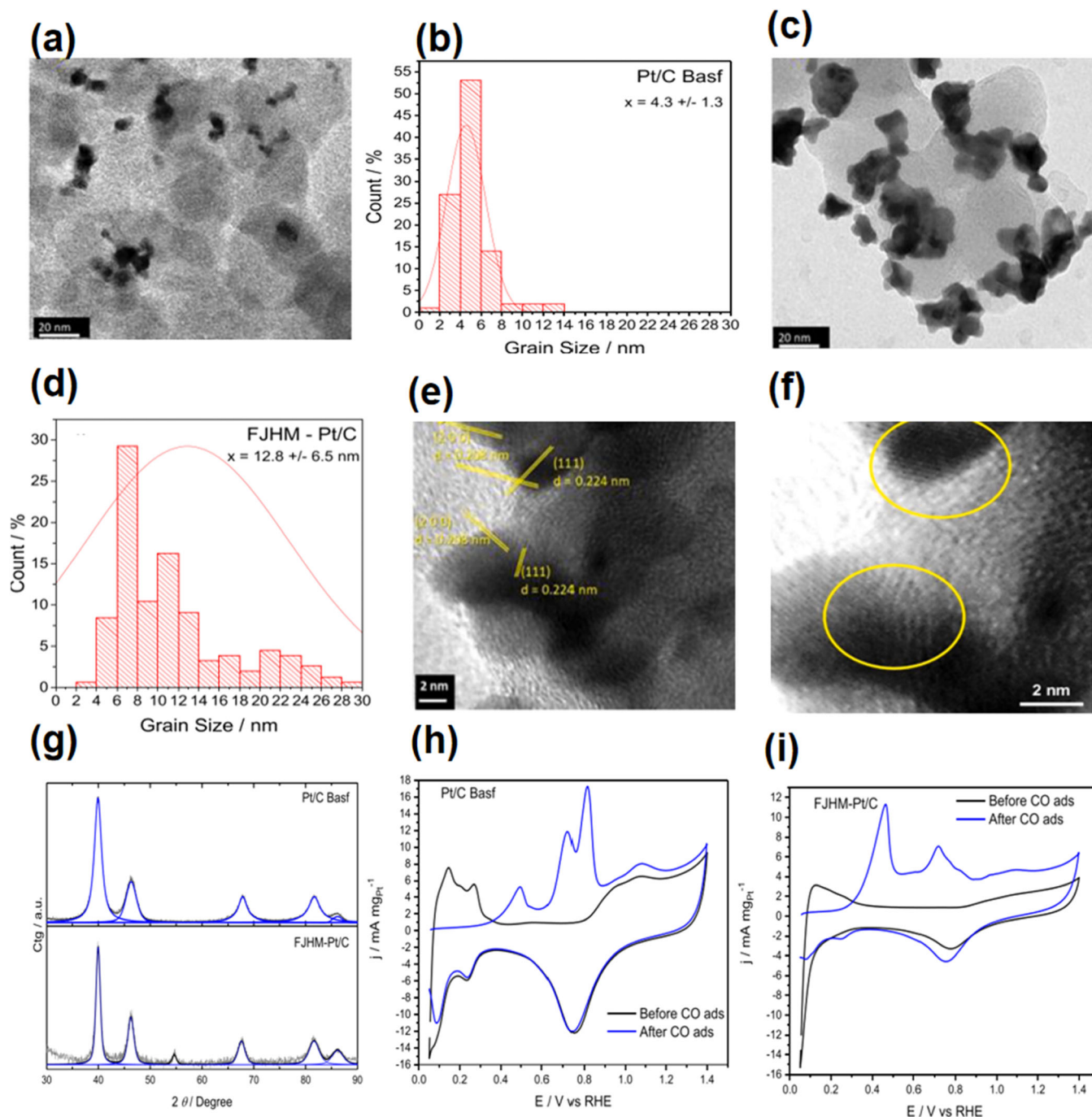


**FIGURE 18** | (a) TEM image of Pt/C BASF. (b) Pt particle size distribution of Pt/C BASF. (c) TEM image of FJHM-Pt/C. (d) Pt particle size distribution of FJHM-Pt/C. (e) TEM image of FJHM-Pt/C with d-spacings highlighted. (f) Interplanar crossings in FJHM-Pt/C. (g) XRD pattern of Pt/C BASF and FJHM-Pt/C. (h, i) Cyclic voltammetry of Pt/C BASF and FJHM-Pt/C. Reproduced under terms of the CC-BY license [125]. Copyright 2024, Julio Nandenha et al., published by Elsevier B.V. on behalf of ESG.

Enhancing the interaction between deposited catalysts and the carbon substrate represents a significant challenge in advancing carbon-based materials for fuel cell anodes. Li et al. have pioneered a rapid heating-cooling method to synthesize carbon-coated Ni nanoparticles, which serve as high-performance perovskite fuel catalysts supported on a RGO substrate (nano-Ni@C/RGO) (Figure 19) [123]. The stable anchoring of Ni nanoparticles resulted in an exceptionally high electroactive specific surface area. It is a promising anode material for direct peroxide-peroxide fuel cells (DPPFCs). This innovative heating

technique holds potential for the synthesis of various other nanoparticles, broadening its applications in energy conversion and storage. Cheng et al. proposed a fast Joule-heated pyrolysis method in which polyaniline (containing C, N) and  $\text{FeCl}_3$ -doped carbon fiber cloth (CFC) were powered at a fixed direct current (DC) voltage [126]. It has excellent performance as the anode and cathode of DPPFC.

In summary, current research has demonstrated the feasibility and potential of HTS technology in the development of fuel cell

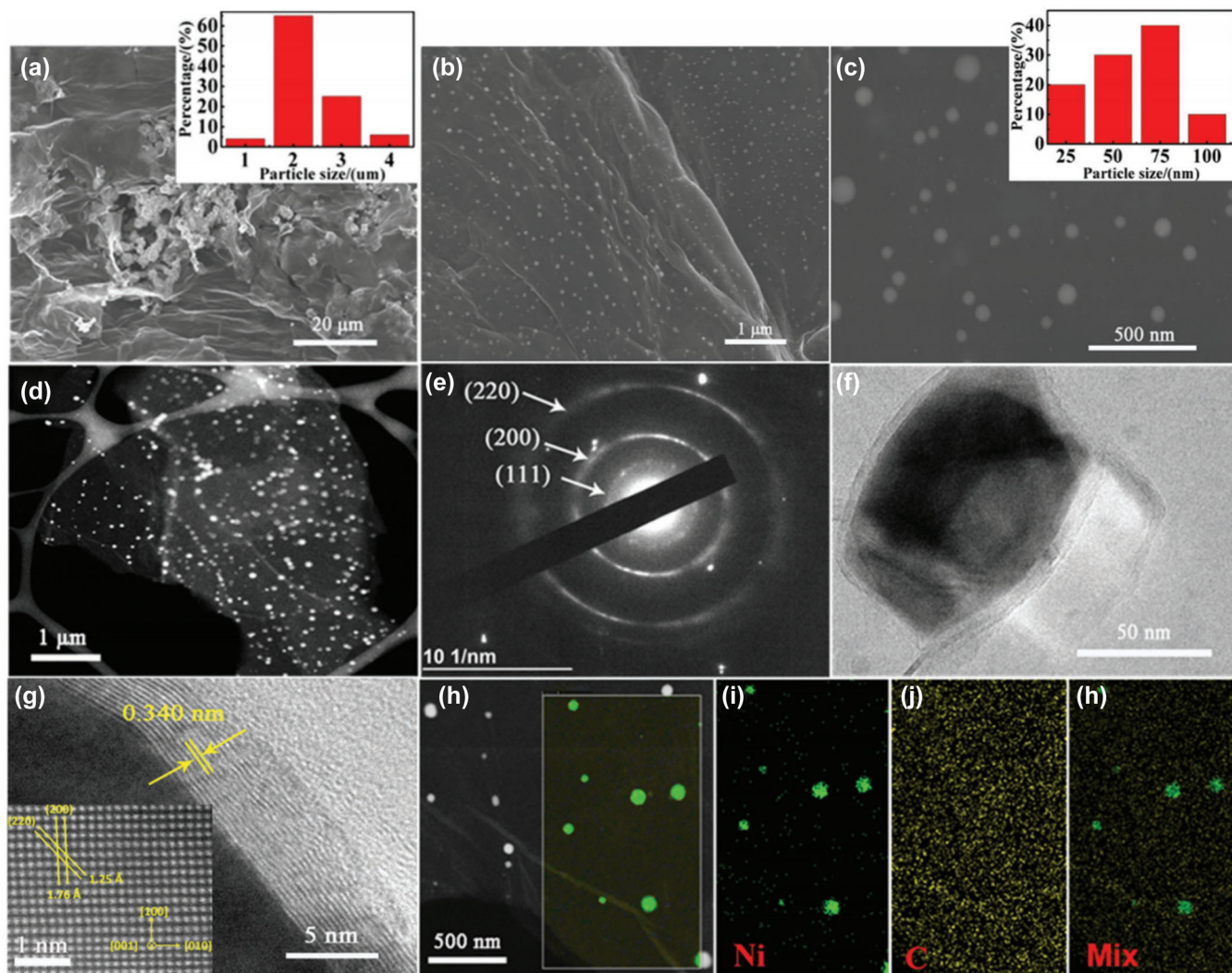


**FIGURE 19** | (a–k) SEM, TEM, and STEM images of nano-Ni@C/RGO, respectively. Reproduced with permission: Copyright 2017, Wiley-VCH GmbH [123].

electrodes. The ultrahigh processing temperatures and ultra-fast heating and cooling rates of HTS technique promote the construction and optimization of high-performance, stable, scalable, and affordable carbon-based material for fuel cell electrodes.

#### 4 | Conclusion

In this report, we presented a comprehensive review of carbon-based materials prepared via the high-temperature shock technique and their applications in the field of electrochemistry, particularly those energy-related processes. First, HTS technique was briefly introduced, covering its history of development, relevant instruments, the synthesis process, the heating principle, and temperature measurement principle. Then the synthesis mechanism of carbon-based nanomaterials via HTS was discussed, based on which principles for precise engineering of the structure, morphology, and composition of synthesized electrocatalysts were derived. In a typical HTS synthesis, the reaction is driven by the high temperature, while the rapid heating and cooling effectively inhibits the growth of nanoparticles via agglomeration or aggregation. Moreover, HTS

enables fine-tuning of carbon vacancies that may further drive phase transitions, formation and preservation of metastable phases that may exhibit high catalytic activities, engineering of carbon and other defects that may act as active centers, induction of synergies between constituents through doping or compounding, and adjustment of the interactions between loaded catalysts and carbon substrates, for optimized electrocatalytic performance.

Despite tremendous application prospects of HTS-derived carbon-based materials in energy-related electrochemical applications that have been demonstrated by numerous studies, there is still enormous space for their improvement in future explorations. We recommend the following directions:

1. Carbon-based nanomaterials synthesized via HTS have been widely applied in the field of electrochemistry. At present, researchers mainly focus on the synthesis and optimization of several common carbon substrates including graphite, carbon fiber, and amorphous carbon. They may explore the synthesis with a wider range of carbon materials, such as other allotropes of carbon, carbonized biomass, and so on.

- At present, HTS syntheses are mainly demonstrated for laboratory-scale preparation of electrocatalysts or electrodes, which are mostly for proof-of-concepts. It is worth attempting to develop large-scale HTS synthesis of carbon-based materials with improved electrochemical performance and affordability.
- There are still challenges in improving the structural diversity of the substrates and obtained catalysts, increasing metal/catalyst loading without altering the catalyst structure, and enhancing the heating and cooling behaviors of the HTS technique itself.
- At present, the improvement of HTS preparation of carbon-based nanomaterials mainly focuses on the loading materials. We can try using HTS to develop and improve carbon substrates, such as transforming them into hollow structures. Special carbon substrates have a large specific surface area, good conductivity, and excellent material transport properties, which can provide more active sites and faster reaction kinetics for electrochemical reactions. They have broad application prospects in electrochemical devices such as supercapacitors, lithium-ion batteries, and fuel cells.
- Due to the fact that HTS is a new technology developed in the past decade, the preparation of carbon-based nanomaterials using HTS has not yet fully covered all fields of electrocatalysis. There are still shortcomings in the research and application of UOR, GOR, benzene series oxidation reaction, AOR, and so on. Researchers can strive to apply HTS-synthesized carbon-based nanomaterials in the above-mentioned fields.
- Because the synthesis process of HTS is millisecond level, the rapid process results in the reaction process not being observed in time. More and more researchers have been committed to applying advanced in situ characterization techniques to explore this, which has the potential to be addressed in the future.

In summary, HTS technology, as an emerging synthesis technique in recent years, plays an important role in accelerating the rational design and preparation of carbon-based nanomaterials for enhanced catalytic performance in various electrochemical applications.

#### Author Contributions

**He Zhu and Si Lan:** conceived conceptualization, methodology, writing—review and editing, supervision, project administration, and funding acquisition. **Wen Huang and Xindong Zhu:** methodology, performed formal analysis, investigation, and writing the original draft. **Zhihua Wang and Haoran Yu:** participated in data curation, formal analysis, writing—review and editing. **Qi Liu and Yu Shao:** assisted in the formal analysis.

#### Acknowledgments

This study was financially supported by the National Key R&D Program of China (No. 2021YFB3802800), the National Natural Science Foundation of China (Nos. 22275089, 52222104, 12261160364), the Fundamental Research Funds for the Central Universities (No. 30922010307).

#### Conflicts of Interest

The authors declare no conflicts of interest.

#### References

- International Energy Agency, International Renewable Energy Agency, United Nations Statistics Division, World Bank, World Health Organization, Tracking SDG 7., *Energy Progress Report 2022* (Washington, DC: World Bank, 2022).
- A. Bueno-López, A. García-García, M. J. Illán-Gómez, A. Linares-Solano, and C. Salinas-Martínez de lecea, "Advances in Potassium Catalyzed Noxreduction by Carbon Materials: An Overview," *Industrial & Engineering Chemistry Research* 46 (2007): 3891–3903.
- D. Liu, L. Dai, X. Lin, et al., "Chemical Approaches to Carbon-Based Metal-Free Catalysts," *Advanced Materials* 31 (2019): 1804863.
- D. Liu, L. Shi, Q. Dai, et al., "Functionalization of Carbon Nanotubes for Multifunctional Applications," *Trends in Chemistry* 6 (2024): 186–210.
- M. Ghorbani, O. Seyedin, and M. Aghamohammadhassan, "Adsorptive Removal of Lead (II) Ion From Water and Wastewater Media Using Carbon-Based Nanomaterials as Unique Sorbents: A Review," *Journal of Environmental Management* 254 (2020): 109814.
- M. Mehmandoust, G. Li, and N. Erk, "Biomass-Derived Carbon Materials as an Emerging Platform for Advanced Electrochemical Sensors: Recent Advances and Future Perspectives," *Industrial & Engineering Chemistry Research* 62 (2023): 4628–4635.
- F. Liu, L. Shi, X. Lin, et al., "Fe/Co Dual Metal Catalysts Modulated by S-Ligands for Efficient Acidic Oxygen Reduction in PEMFC," *Science Advances* 9 (2023): eadg0366.
- L. Shi, D. Liu, X. Lin, et al., "Stable and High-performance Flow H<sub>2</sub>-O<sub>2</sub> Fuel Cells With Coupled Acidic Oxygen Reduction and Alkaline Hydrogen Oxidation Reactions," *Advanced Materials* 36 (2024): 2314077.
- P. Serp and B. Machado, *Royal Society of Chemistry, Royal Society of Chemistry* (Cambridge, UK: Nanostructured Carbon Materials for Catalysis, 2015).
- A. B. Jorge, R. Jervis, A. P. Periasamy, et al., "3D Carbon Materials for Efficient Oxygen and Hydrogen Electrocatalysis," *Advanced Energy Materials* 10 (2020): 1902494.
- F. J. Rodríguez-Varela, F. Javier, and T. W. Napporn, *Advanced Electrocatalysts for Low-Temperature Fuel Cells* (Berlin: Springer, 2018).
- X. Liu, N. Fechner, M. Antonietti, M. G. Willinger, and R. Schlögl, "Synthesis of Novel 2-d Carbon Materials: Sp<sub>2</sub> Carbon Nanoribbon Packing to Form Well-Defined Nanosheets," *Materials Horizons* 3 (2016): 214–219.
- Y. Yao, Q. Xiao, M. Kawaguchi, T. Tsuda, H. Yamada, and S. Kuwabata, "Impact of Sp<sub>2</sub> Carbon Material Species on Pt Nanoparticle-Based Electrocatalysts Produced by One-Pot Pyrolysis Methods With Ionic Liquids," *RSC Advances* 12 (2022): 14268–14277.
- K. Satendra, G. Manoj, S. Netrapal, N. Sathish, and K. Surender, "A Comprehensive Review of the 3D Printing of Sp<sub>2</sub> Carbons: Materials, Properties and Applications," *Carbon* 203 (2023): 897.
- P. R. Unwin, A. G. Güell, and G. Zhang, "Nanoscale Electrochemistry of Sp<sub>2</sub> Carbon Materials: From Graphite and Graphene to Carbon Nanotubes," *Accounts of Chemical Research* 49 (2016): 2041–2048.
- J. Luan, W.-L. Duan, Y.-X. Li, et al., "Metal–Organic Framework as Catalyst Precursor of Floating Catalyst Chemical Vapor Deposition for Single-Walled Carbon Nanotube Manufacture," *ACS Sustainable Chemistry & Engineering* 11 (2023): 12423–12434.
- C. Chen, C. Luo, Y. Jin, J. Li, Q. Zhao, and W. Yang, "Short-Process Spray-Drying Synthesis of Lithium Iron Phosphate@Carbon Composite for Lithium-Ion Batteries," *ACS Sustainable Chemistry & Engineering* 12 (2024): 14077–14086.



18. G. Gečė, J. Pilipavičius, N. Traškina, A. Drabavičius, and L. Vilčiauskas, "Solvothermal Engineering of  $\text{NaTi}_2(\text{PO}_4)_3$  Nanomorphology for Applications in Aqueous Na-Ion Batteries," *ACS Sustainable Chemistry & Engineering* 11 (2023): 3429–3436.
19. Z. Pang, X. Xiong, F. Tian, et al., "A Sustainable Molten Salt Leaching-Electrodeposition Route Toward Converting Rice Husks Into Functional Silicon Nanowires and Porous Carbon," *ACS Sustainable Chemistry & Engineering* 12 (2024): 7200–7210.
20. R. Gusain, N. Kumar, and S. S. Ray, "Recent Advances in Carbon Nanomaterial-Based Adsorbents for Water Purification," *Coordination Chemistry Reviews* 405 (2020): 213111.
21. Z. Yang, J. Tian, Z. Yin, C. Cui, W. Qian, and F. Wei, "Carbon Nanotube- and Graphene-Based Nanomaterials and Applications in High-Voltage Supercapacitor: A Review," *Carbon* 141 (2019): 467–480.
22. X.-T. Yan, *Chemical Vapour Deposition: An Integrated Engineering Design for Advanced Materials* (London: Springer Nature, 2010).
23. A. C. Jones and L. H. Michael, *Chemical Vapour Deposition: Precursors, Processes and Applications* (Cambridge: Royal Society of Chemistry, 2008).
24. M. Malamataris, A. Charisi, S. Malamataris, K. Kachrimanis, and I. Nikolakis, "Spray Drying for the Preparation of Nanoparticle-Based Drug Formulations as Dry Powders for Inhalation," *Processes* 8 (2020): 788.
25. R. Ghosh Chaudhuri and S. Paria, "Core/Shell Nanoparticles: Classes, Properties, Synthesis Mechanisms, Characterization, and Applications," *Chemical Reviews* 112 (2012): 2373–2433.
26. S. Keshani, W. R. W. Daud, M. M. Nourouzi, F. Namvar, and M. Ghasemi, "Spray Drying: An Overview on Wall Deposition, Process and Modeling," *Journal of Food Engineering* 146 (2015): 152–162.
27. F. Wu, H. Zhang, W. Lu, and X. Li, "Synthesis of  $\text{ZnO/CuO}$  Composite Coaxial Nanoarrays by Combined Hydrothermal-Solvothermal Method and Potential for Solar Cells," *Journal of Composite Materials* 49 (2015): 2009–2014.
28. L. Bai, K. Zhu, J. Qiu, R. Zhu, H. Gu, and H. Ji, "Synthesis of (K,Na)  $\text{NbO}_3$  Particles by Traditional Hydrothermal Method and High-Temperature Mixing Method Under Hydrothermal-Solvothermal Conditions," *Research on Chemical Intermediates* 37 (2011): 185–193.
29. S. Dou, J. Xu, X. Cui, et al., "High-Temperature Shock Enabled Nanomanufacturing for Energy-Related Applications," *Advanced Energy Materials* 10 (2020): 2001331.
30. Y. Yao, Z. Huang, T. Li, et al., "High-Throughput, Combinatorial Synthesis of Multimetallic Nanoclusters," *Proceedings of the National Academy of Sciences United States of America* 117 (2020): 6316–6322.
31. G. Chen, J. Zheng, L. Liu, et al., "Application of Microfluidics in Wearable Devices," *Small Methods* 3 (2019): 1900050.
32. M. Cui, C. Yang, S. Hwang, et al., "Multi-Principal Elemental Intermetallic Nanoparticles Synthesized via a Disorder-to-Order Transition," *Science Advances* 8 (2022): eabm4322.
33. H. J. Hwang, J. Koo, M. Park, N. Park, Y. Kwon, and H. Lee, "Multilayer Graphynes for Lithium Ion Battery Anode," *Journal of Physical Chemistry C* 117 (2013): 6919–6923.
34. J. Li, L. Huang, D. Duan, X. Li, H. Song, and S. Liao, "Biogelatin-Derived and N,S-Codoped 3D Network Carbon Materials Anchored With  $\text{RuO}_2$  as an Efficient Cathode for Rechargeable  $\text{Li-O}_2$  Batteries," *Journal of Physical Chemistry C* 125 (2021): 21914–21921.
35. C. T. Alexander, A. M. Abakumov, R. P. Forslund, K. P. Johnston, and K. J. Stevenson, "Role of the Carbon Support on the Oxygen Reduction and Evolution Activities in  $\text{LaNiO}_3$  Composite Electrodes in Alkaline Solution," *ACS Applied Energy Materials* 1 (2018): 1549–1558.
36. J. Yang, S. H. Kim, S. K. Kwak, and H.-K. Song, "Curvature-Induced Metal-Support Interaction of Anislands-by-Islands composite of Platinum Catalyst and Carbon Nano-Onion for Durable Oxygen Reduction," *ACS Applied Materials & Interfaces* 9 (2017): 23302–23308.
37. Y. Cui, Y. Cheng, C. Yang, et al., "High-Performance Electrocatalytic  $\text{CO}_2$  Reduction for CO Generation Using Hydrophobic Porous Carbon Supported Au," *ACS Sustainable Chemistry & Engineering* 11 (2023): 11229–11238.
38. S. Hoekx, N. Daems, D. Arenas Esteban, S. Bals, and T. Breugelmans, "Toward the Rational Design of Cu Electrocatalysts for Improved Performance of the  $\text{NO}_3\text{RR}$ ," *ACS Applied Energy Materials* 7 (2024): 3761–3775.
39. S. Lu, M. Hummel, Z. Gu, et al., "Highly Efficient Urea Oxidation via Nesting Nano-Nickel Oxide in Eggshell Membrane-Derived Carbon," *ACS Sustainable Chemistry & Engineering* 9 (2021): 1703–1713.
40. J. Vidal Laveda, J. E. Low, F. Pagani, et al., "Stabilizing Capacity Retention in NMC811/Graphite Full Cells via TMSPI Electrolyte Additives," *ACS Applied Energy Materials* 2 (2019): 7036–7044.
41. A. J. de Mello, M. Habgood, N. L. Lancaster, T. Welton, and R. C. R. Wootton, "Precise Temperature Control in Microfluidic Devices Using Joule Heating of Ionic Liquids," *Lab on a Chip* 4 (2004): 417.
42. C. B. Sweeney, M. L. Burnette, M. J. Pospisil, et al., "Dielectric Barrier Discharge Applicator for Heating Carbon Nanotube-Loaded Interfaces and Enhancing 3D-Printed Bond Strength," *Nano Letters* 20 (2020): 2310–2315.
43. X. Cui, Y. Liu, and Y. Chen, "Ultrafast Micro/Nano-Manufacturing of Metastable Materials for Energy," *National Science Review* 11 (2024): nwae033.
44. J. Li, C. Wang, X. Chen, et al., "Flash Synthesis of Ultrafine and Active NiRu Alloy Nanoparticles on N-Rich Carbon Nanotubes via Joule Heating for Efficient Hydrogen and Oxygen Evolution Reaction," *Journal of Alloys and Compounds* 959 (2023): 170571.
45. D. C. Marcano, D. V. Kosynkin, J. M. Berlin, et al., "Improved Synthesis of Graphene Oxide," *ACS Nano* 4 (2010): 4806–4814.
46. Y. Li, X. Shu, W. Ma, J. Zhou, X. Bai, and Q. Zhang, "Introduction and Characterization of Vacancies in Semiconductor Materials and Their Impact on Photocatalysis," *Journal of Functional Materials* 53 (2022): 11015.
47. J. Zhang, "Research on Flexible Screen Based on Graphene Composite Materials," *China Chemical Trade* 35 (2017): 224.
48. B. V. Politov, A. Y. Suntsov, I. A. Leonidov, M. V. Patrakeev, and V. L. Kozhevnikov, "High-Temperature Defect Thermodynamics of Nickel Substituted Double-Perovskite Cobaltite  $\text{PrBaCo}_{2-x}\text{Ni}_x\text{O}_{6-x}$  ( $x = 0.2$ )," *Journal of Alloys and Compounds* 727 (2017): 778–784.
49. P. K. Kofstad, Ø. Johannesen, and A. G. Andersen, *Selected Topics in High Temperature Chemistry: Defect Chemistry of Solids* (Amsterdam: Elsevier Science, 1989).
50. Y. Wang, Y. Chen, S. D. Lacey, et al., "Reduced Graphene Oxide Film With Record-High Conductivity and Mobility," *Materials Today* 21 (2018): 186–192.
51. Y. Yao, Z. Huang, P. Xie, et al., "Carbothermal Shock Synthesis of High-Entropy-Alloy Nanoparticles," *Science* 359 (2018): 1489–1494.
52. J. Ahn, S. Park, D. Oh, et al., "Rapid Joule Heating Synthesis of Oxide-Socketed High-Entropy Alloy Nanoparticles as  $\text{CO}_2$  Conversion Catalysts," *ACS Nano* 17 (2023): 12188–12199.
53. B. Deng, Z. Wang, W. Chen, et al., "Phase Controlled Synthesis of Transition Metal Carbide Nanocrystals by Ultrafast Flash Joule Heating," *Nature Communications* 13 (2022): 262.
54. W. Chen, J. T. Li, Z. Wang, et al., "Ultrafast and Controllable Phase Evolution by Flash Joule Heating," *ACS Nano* 15 (2021): 11158–11167.
55. M. Li, Z. Hu, H. Li, et al., "Pt–Ni Alloy Nanoparticles via High-Temperature Shock as Efficient Electrocatalysts in the Oxygen Reduction Reaction," *ACS Applied Nano Materials* 5 (2022): 8243–8250.

56. Y. Song, J. Di, C. Zhang, et al., "Millisecond Tension-Annealing for Enhancing Carbon Nanotube Fibers," *Nanoscale* 11 (2019): 13909–13916.
57. Z. Huang, Y. Yao, Z. Pang, et al., "Direct Observation of the Formation and Stabilization of Metallic Nanoparticles on Carbon Supports," *Nature Communications* 11 (2020): 6373.
58. X. Lin, W. Zhao, W. Zhou, et al., "Epitaxial Growth of Aligned and Continuous Carbon Nanofibers From Carbon Nanotubes," *ACS Nano* 11 (2017): 1257–1263.
59. X. Yang, C. P. Nielsen, S. Song, and M. B. McElroy, "Breaking the Hard-to-Abate Bottleneck in China's Path to Carbon Neutrality With Clean Hydrogen," *Nature Energy* 7 (2022): 955–965.
60. H. Cui, D. Zhang, Z. Wu, et al., "Tailoring Hydroxyl Groups of Organic Phenazine Anodes for High-Performance and Stable Alkaline Batteries," *Energy & Environmental Science* 17 (2024): 114–122.
61. Z. Zhu, T. Jiang, M. Ali, et al., "Rechargeable Batteries for Grid Scale Energy Storage," *Chemical Reviews* 122 (2022): 16610–16751.
62. H. Zhang, C. Li, G. G. Eshetu, et al., "From Solid-Solution Electrodes and the Rocking-Chair Concept to Today's Batteries," *Angewandte Chemie International Edition* 59 (2020): 534–538.
63. Z. Zhang, Y. Song, B. Zhang, L. Wang, and X. He, "Metallized Plastic Foils: A Promising Solution for High-Energy Lithium-Ion Battery Current Collectors," *AEnM* 13 (2023): 202302134.
64. P. Liu, Z. Qiu, F. Cao, et al., "Liquid-Source Plasma Technology for Construction of Dual Bromine-Fluorine-Enriched Interphases on Lithium Metal Anodes With Enhanced Performance," *Journal of Materials Science & Technology* 177 (2024): 68–78.
65. N. Zhu, Y. Yang, Y. Li, Y. Bai, J. Rong, and C. Wu, "Carbon-Based Interface Engineering and Architecture Design for High-Performance Lithium Metal Anodes," *Carbon Energy* 6 (2024): e423.
66. S. Chen, Z. Wang, M. Zhang, et al., "Practical Evaluation of Pre-lithiation Strategies for Next-Generation Lithium-ion Batteries," *Carbon Energy* 5 (2023): e323.
67. W. Zhang, X. Wei, T. Wu, et al., "Carbothermal Shock Enabled Functional Nanomaterials for Energy-Related Applications," *Nano Energy* 118 (2023): 108994.
68. C. Li, C. Zheng, F. Cao, Y. Zhang, and X. Xia, "The Development Trend of Graphene Derivatives," *Journal of Electronics* 51 (2022): 4107.
69. L. Huang, T. Guan, H. Su, et al., "Synergistic Interfacial Bonding in Reduced Graphene Oxide Fiber Cathodes Containing Polypyrrole@sulfur Nanospheres for Flexible Energy Storage," *Angewandte Chemie International Edition* 61 (2022): e202212151.
70. D. A. Habtom, A. Kotronia, N. Garcia-Araez, K. Edström, and D. Brandell, "Charting the Course to Solid-State Dual-ion Batteries," *Carbon Energy* 6 (2024): e425.
71. P. Huang, Z. Li, L. Chen, et al., "Ultrafast Dual-Shock Chemistry Synthesis of Ordered/Disordered Hybrid Carbon Anodes: High-Rate Performance of Li-Ion Batteries," *ACS Nano* 18 (2024): 18344–18354.
72. W. Chen, R. V. Salvatierra, J. T. Li, et al., "Flash Recycling of Graphite Anodes," *Advanced Materials* 35 (2023): 202207303.
73. Y. Chen, Y. Li, Y. Wang, et al., "Rapid, In Situ Synthesis of High Capacity Battery Anodes Through High Temperature Radiation-Based Thermal Shock," *Nano Letters* 16 (2016): 5553–5558.
74. S. Liu, B. Liu, M. Liu, et al., "Rapid, In Situsynthesis of Ultra-Small Silicon Particles for Boosted Lithium Storage Capability Through Ultrafast Joule Heating," *Nanoscale* 16 (2024): 2531–2539.
75. F. Yang, P. Deng, H. He, et al., "Rapid Joule Heating-Induced Welding of Silicon and Graphene for Enhanced Lithium-Ion Battery Anodes," *Chemical Engineering Journal* 494 (2024): 152828.
76. S. Liu, B. Liu, Z. Yu, et al., "Rapid Release of Silicon by Ultrafast Joule Heating Generates Mechanically Stable Shell-Shell Si/C Anodes With Dominant Inward Deformation," *ACS Nano* 18 (2024): 17326–17338.
77. H. Wu, H. Wen, C. Wang, et al., "Tailored Yolk-Shell Design to Silicon Microparticles via Scalable and Template-Free Synthesis for Superior Lithium Storage," *Small* 20 (2024): 202311779.
78. P. Li, Z. Fang, X. Dong, C. Wang, and Y. Xia, "The Pathway Toward Practical Application of Lithium-Metal Anodes for Non-Aqueous Secondary Batteries," *National Science Review* 9 (2022): nwac031.
79. C. P. Yang, Y. G. Yao, S. M. He, H. Xie, E. Hitz, and L. B. Hu, *Advanced Materials* 29 (2017): 1702714.
80. X. Shan, J. Zhu, Z. Qiu, et al., "Ultrafast-Loaded Nickel Sulfide on Vertical Graphene Enabled by Joule Heating for Enhanced Lithium Metal Batteries," *Small* 20 (2024): 2401491.
81. W. Zhu, J. C. Zhang, J. W. Luo, et al., "Ultrafast Non-Equilibrium Synthesis of Cathode Materials for Li-Ion Batteries," *Advanced Materials* 35 (2023): 2208974.
82. Z. Liu, J. Zhang, J. Luo, et al., "Approaching Ultimate Synthesis Reaction Rate of Ni-Rich Layered Cathodes for Lithium-Ion Batteries," *Nano-Micro Letters* 16 (2024): 210.
83. Y. Chen, K. Fu, S. Zhu, et al., "Reduced Graphene Oxide Films With Ultrahigh Conductivity as Li-Ion Battery Current Collectors," *Nano Letters* 16 (2016): 3616–3623.
84. H. Pan, Z. Cheng, Z. Zhou, et al., "Boosting Lean Electrolyte Lithium-Sulfur Battery Performance With Transition Metals: A Comprehensive Review," *Nano-Micro Letters* 15 (2023): 165.
85. H. Raza, S. Bai, J. Cheng, et al., "Li-S Batteries: Challenges, Achievements and Opportunities," *Electrochemical Energy Reviews* 6 (2023): 29.
86. Z. Wang, J. Zhang, H. Kang, Y. Liu, M. Wang, and H. Zhang, "Li<sub>1+x</sub>Mn<sub>2</sub>O<sub>4</sub> Synthesized by In-Situ Lithiation for Improving Sulfur Redox Kinetics of Li-S Batteries," *Electrochimica Acta* 404 (2022): 139780.
87. Z. H. Wang, H. Zhu, J. Jiang, et al., "Fence-Type Molecular Electrocatalysts for High-Performance Lithium-Sulfur Batteries," *Angewandte Chemie International Edition English* 63 (2024): e202410823.
88. Y. H. Xu, W. C. Yuan, C. N. Geng, et al., "High-Entropy Catalysis Accelerating Stepwise Sulfur Redox Reactions for Lithium-Sulfur Batteries," *Advancement of Science* 11 (2024): 2402497.
89. G. Wang, T. Tang, K. H. Ye, et al., "Dual Hole Transport Layers Heterojunction and Band Alignment Engineered Mo:BiVO<sub>4</sub> Photoanodes for Efficient Water Splitting (Small 37/2024)," *Small* 20 (2024): 2310801.
90. H. Y. Dong, L. Wang, Y. Cheng, et al., "Flash Joule Heating: A Promising Method for Preparing Heterostructure Catalysts to Inhibit Polysulfide Shuttling in Li-S Batteries," *Advanced Science* 11 (2024): 2405351.
91. W. B. Jung, H. Park, J. S. Jang, et al., "Polyelemental Nanoparticles as Catalysts for a Li-O<sub>2</sub> Battery," *ACS Nano* 15 (2021): 4235–4244.
92. P. G. Bruce, S. A. Freunberger, L. J. Hardwick, and J. M. Tarascon, "Li-O<sub>2</sub> and Li-S Batteries With High Energy Storage," *Nature Materials* 11 (2012): 19–29.
93. Q. Lu, H. Wu, X. R. Zheng, et al., "Encapsulating Cobalt Nanoparticles in Interconnected N-Doped Hollow Carbon Nanofibers With Enriched Co-N-C Moiety for Enhanced Oxygen Electrocatalysis in Zn-Air Batteries," *Advanced Science* 8 (2021): 2101438.
94. M. Xie, X. Xiao, D. Wu, et al., "MOF-Mediated Synthesis of Novel PtFeCoNiMn High-Entropy Nano-Alloy as Bifunctional Oxygen Electrocatalysts for Zinc-Air Battery," *Nano Research* 17 (2024): 5288–5297.
95. B. Lu, X. Wu, M. Zhang, et al., "Steering the Orbital Hybridization to Boost the Redox Kinetics for Efficient Li-CO<sub>2</sub> Batteries," *Journal of the American Chemical Society* 146 (2024): 20814–20822.

96. Y. Liu, J. W. Ma, S. L. Huang, S. Y. Niu, and S. Y. Gao, "Highly Dispersed Copper-Iron Nanoalloy Enhanced Electrocatalytic Reduction Coupled With Plasma Oxidation for Ammonia Synthesis From Ubiquitous Air and Water," *Nano Energy* 117 (2023): 108840.
97. L. Lai, J. Li, Y. Y. Deng, Z. X. Yu, L. Wei, and Y. Chen, "Carbon and Carbon/Metal Hybrid Structures Enabled by Ultrafast Heating Methods," *Small Structure* 3 (2022): 2200112.
98. S. S. Yuan, Y. H. Liu, J. Q. Zheng, M. Y. Cui, K. W. Wang, and N. Li, "Activating Molybdenum Carbide via a Surface Sulfur Modification to Enhance Hydrogen Evolution Activity," *Journal of Alloys and Compounds* 933 (2023): 167664.
99. H. Zhang, S. Qi, K. Zhu, et al., "Ultrafast Synthesis of Mo<sub>2</sub>C-Based Catalyst by Joule Heating Towards Electrocatalytic Hydrogen Evolution Reaction," *Symmetry* 15 (2023): 801.
100. J. Li, C. Wang, X. Chen, et al., "Flash Synthesis of Ultrafine and Active NiRu Alloy Nanoparticles on N-Rich Carbon Nanotubes via Joule Heating for Efficient Hydrogen and Oxygen Evolution Reaction," *Journal of Alloys and Compounds* 959 (2023): 170571.
101. C. Li, Z. Wang, M. Liu, et al., "Ultrafast Self-Heating Synthesis of Robust Heterogeneous Nanocarbides for High Current Density Hydrogen Evolution Reaction," *Nature Communications* 13 (2022): 3338.
102. Y. Liao, R. Zhu, W. Zhang, et al., "Transient Synthesis of Carbon-Supported High-Entropy Alloy Sulfide Nanoparticles via Flash Joule Heating for Efficient Electrocatalytic Hydrogen Evolution," *Nano Research* 17 (2024): 3379–3389.
103. A. Mashhadian, S. W. Wu, Y. Hao, et al., "Rapid Synthesis of Phase-Engineered Tungsten Carbide Electrocatalysts via Flash Joule Heating for High-Current-Density Hydrogen Evolution," *ChemRxiv* (2024): t19wv, <https://doi.org/10.26434/chemrxiv-2024-t19wv>.
104. L. Yang, Y. Yang, S. Wang, X. Guan, X. Guan, and G. Wang, "Multi-Heteroatom-Doped Carbon Materials for Solid-State Hybrid Supercapacitors With a Superhigh Cycling Performance," *Energy & Fuels* 34 (2020): 5032–5043.
105. S. Hou, W. D. Cheng, and F. Guo, *Sustainable Materials and Technologies* 35 (2023): e00570.
106. F. Li, Z. Zhao, X. Chen, et al., "A Review of the Use of MXenes as Hosts in Lithium Metal Anodes and the Anode Formation," *Carbon* 215 (2023): 118444.
107. W. Chen, C. Ge, J. T. Li, et al., "Heteroatom-Doped Flash Graphene," *ACS Nano* 16 (2022): 6646–6656.
108. C. Zhu, W. Yang, J. Di, et al., "CoNi Nanoparticles Anchored Inside Carbon Nanotube Networks by Transient Heating: Low Loading and High Activity for Oxygen Reduction and Evolution," *Journal of Energy Chemistry* 54 (2021): 63–71.
109. P. Li, W. Wei, J. Li, et al., "Flash Joule Heating Synthesis of Carbon Supported Ultrafine Metallic Heterostructures for High-Performance Overall Water Splitting," *Journal of Alloys and Compounds* 947 (2023): 169630.
110. G. B. Chen, R. H. Lu, C. Z. Li, et al., "Hierarchically Porous Carbons With Highly Curved Surfaces for Hosting Single Metal FeN<sub>4</sub> Sites as Outstanding Oxygen Reduction Catalysts," *Advanced Materials* 35 (2023): 2300907.
111. M. Inagaki, M. Toyoda, Y. Soneda, and T. Morishita, "Nitrogen-Doped Carbon Materials," *Carbon* 132 (2018): 104–140.
112. X. Zhang, G. Han, and S. Zhu, "Flash Nitrogen-Doped Carbon Nanotubes for Energy Storage and Conversion," *Small* 20 (2024): 2305406.
113. Z. Y. Hu, L. Huang, M. Y. Ma, et al., "A Quick Joule-Heating Coupled With Solid-Phase Synthesis for Carbon-Supported Pd–Se Nanoparticles Toward High-Efficiency Electrocatalysis," *Advanced Functional Materials* 34 (2024): 2405945.
114. B. Wulan, X. Y. Cao, D. X. Tan, J. Z. Ma, and J. Z. Zhang, "To Stabilize Oxygen on In/In<sub>2</sub>O<sub>3</sub> Heterostructure via Joule Heating for Efficient Electrocatalytic CO<sub>2</sub> Reduction," *Advanced Functional Materials* 33 (2024): 2209114.
115. M. Wang, H. Wang, Y. Gu, et al., "In Situ Generation of Flash Graphene Supported Spherical Bismuth Nanoparticles in Less Than 200 ms for Highly Selective Carbon Dioxide Electroreduction," *ACS Materials Letters* 6 (2024): 100–108.
116. W. T. Zhang, X. Q. Wang, F. Q. Zhang, et al., "Frontiers in High Entropy Alloys and High Entropy Functional Materials," *Rare Metals* 43 (2024): 4639–4776.
117. D. W. Xi, J. Y. Li, J. X. Low, et al., "Limiting the Uncoordinated N Species in M–N<sub>x</sub> Single-Atom Catalysts Toward Electrocatalytic CO<sub>2</sub> Reduction in Broad Voltage Range," *Advanced Materials* 34 (2022): 2104090.
118. Z. Zhang, Y. Liu, X. Su, et al., "Electro-Triggered Joule Heating Method to Synthesize Single-Phase Cuni Nano-Alloy Catalyst for Efficient Electrocatalytic Nitrate Reduction Toward Ammonia," *Nano Research* 16 (2023): 6632–6641.
119. W. X. Tao, P. F. Wang, H. Li, R. Huang, and G. Zhou, "Engineering Sulfur Vacancies Optimization in Ni<sub>3</sub>Co<sub>6</sub>S<sub>8</sub> Nanospheres Toward Extraordinarily Efficient Nitrate Electroreduction to Ammonia," *Applied Catalysis B: Environment* 324 (2023): 122193.
120. C. Kim, J. Y. Song, C. Choi, et al., "Atomic-Scale Homogeneous Ru–Cu Alloy Nanoparticles for Highly Efficient Electrocatalytic Nitrogen Reduction," *Advanced Materials* 34 (2022): 2205270.
121. Y. Wang, Y. Pang, H. Xu, A. Martinez, and K. S. Chen, "PEM Fuel Cell and Electrolysis Cell Technologies and Hydrogen Infrastructure Development—A Review," *Energy & Environmental Science* 15 (2022): 2288–2328.
122. P. Prabhu, V. Jose, and J. M. Lee, "Heterostructured Catalysts for Electrocatalytic and Photocatalytic Carbon Dioxide Reduction," *Advanced Functional* 30 (2020): 1910768.
123. Y. Li, Y. Chen, A. Nie, et al., "In Situ, Fast, High-Temperature Synthesis of Nickel Nanoparticles in Reduced Graphene Oxide Matrix," *Advanced Energy Materials* 7 (2017): 1601783.
124. Y. Y. Deng, H. Liu, L. Lai, et al., "Platinum-Ruthenium Bimetallic Nanoparticle Catalysts Synthesized via Direct Joule Heating for Methanol Fuel Cells," *Small* (2024): 2403967, <https://doi.org/10.1002/sml.202403967>.
125. J. Nandeha, G. Silvestrin, L. Otubo, et al., "Enhanced Carbon Monoxide Tolerance of Platinum Nanoparticles Synthesized Through the Flash Joule Heating Method," *International Journal of Electrochemistry* 19 (2024): 100585.
126. W. Cheng, S. Hou, and F. Guo, "Joule-Heating Pyrolysis-Derived Fe, N Co-Doped Carbon and Its Performance in Direct Peroxide-Peroxide Fuel Cells," *Journal of the Electrochemical Society* 169 (2022): 094506.